SINGLE EVENT EFFECT TESTS WITH LASER AND ION BEAM

by

F. BELGİN ERGİN

THESIS SUBMITTED TO
THE GRADUATE SCHOOL OF NATURAL AND APPLIED SCIENCES
OF
THE ABANT İZZET BAYSAL UNIVERSITY
IN PARTIAL FULFILLMENT OF THE REQUIREMENTS FOR THE
DEGREE OF
MASTER OF SCIENCE
IN
THE DEPARTMENT OF PHYSICS

DECEMBER 2011

Approval of the Graduate School of Natural and Applied Sciences

Prof. Dr. Nihat Çelebi

Director

I certify that this thesis satisfies all the requirements as a thesis for the degree of Master of Science.

Prof. Dr. Kıvılcım Kılıç

Head of Physics Department

This is to certify that we have read this thesis and that in our opinion it is fully adequate, in scope and quality as a thesis for the degree of Master of Science.

Prof. Dr. Behçet Alpat

Co-Supervisor

Assoc. Prof. Dr. Haluk Denizli

Supervisor

Examining Committee Members

1. Assoc. Prof. Dr. Haluk Denizli .....

2. Assist. Prof. Dr. Ercan Piliçer .....

3. Assist. Prof. Dr. Hakan Yetiş .....

To My Family ...

ACKNOWLEDGEMENTS

The work presented in this thesis could not have been done without any help, support and motivation of many people. But the first person, I would like to thank my supervisor Assoc. Prof. Haluk Denizli, for his constant support, challenging and encouragement during the development of this thesis. I would like to thank all staff from MAPRad group, especially the head of MAPRAD group who is my co-supervisor Prof. Dr. Behçet Alpat for valuable opportunity. Of course, I am deeply greatful to Dr. Ercan Piliçer for his endless support, guidance and sharing dicussions during the preperation of this thesis. I would like to greatfully thank for their patient and support to Gülay Göksu and other friends from Perugia,research assistants Arzu Kurt and Ali Yılmaz from Abant Izzet Baysal University, Bolu and Nagihan Osmanca, Betül Çelik for their motivation even in the worst times. Finally, never enough but I want to dedicate this thesis to especially my family for their endless support, enthusiasm and love.

ABSTRACT

SINGLE EVENT EFFECT TESTS WITH LASER AND ION BEAM

Ergin, F. Belgin

Master of Science, Department of Physics

Supervisor: Assoc. Prof. Dr. Haluk Denizli

Co-Supervisor: Prof. Dr. Behçet Alpat

December 2011, 69 pages

Single Event Effect (SEE) is a process which is generated by heavy ions and protons. While heavy ions and protons pass through semiconductor based electronic devices like CMOS (Complementary Metal Oxide Semiconductor), optoelectronic or bipolar electronic devices, depending on their energy and type, may create parasitic transistors causing soft (not distructive) or hard (potentially distructive) errors. For this reason, these devices have to be tested on Earth for their susceptibility to radiation effects. The extended to which the devices are to be tested depends on several factors as mission duration, location and device's use. The test standarts are provided by space agencies such as NASA and ESA in which the test procedures are described in detail. To analyse the radiation environment for a given set of mission parameters, SPENVIS, ĆREME96, and ÓMERE are the most commonly used information systems or tools. The qualification test aganist SEE is performed at heavy ion and proton accelerators as LNS (Laboratori Nazionali del Sud'). An infirared pulsed laser system developed in MAPRAD laboratories is a useful tool for qualitative measurements. Several devices were tested

first at IR laser beam setup and then were taken to LNS laboratories for testing with heavy ions. In this work, we investigated the setups, which are used for laser beam test and ion beam test, in detail and their simulations were developed with different simulation programs before the devices were tested by ion beams. Used simulation programs GEANT4 and FLUKA for these simulations, some parameters were calculated such as LET (Linear Energy Transfer), deposited energy and track length etc. The results of the simulations were compared and discussed.

Keywords: Radiation hardness test, GEANT 4, FLUKA, Linear Energy Transfer (LET)

ÖZET

TEK OLAY ETKİSİNİN İYON DEMETLERİ VE LAZER İLE TEST EDİLMESİ

Ergin, F. Belgin

Yüksek Lisans, Fizik Bölümü

Tez Danışmanı: Doç. Dr. Haluk Denizli

Ortak Tez Danışmanı: Prof. Dr. Behçet Alpat

December 2011, 69 sayfa

Tek olay etkisi ağır iyonlar ve protonlar tarafından meydana gelen bir olaydır. Ağır iyonlar ve protonlar yarıiletken tabanlı CMOS, optoelektronik, bipolar transistörler gibi elektronik cihazlardan geçerken, enerjilerine ve türlerine bağlı olarak kalıcı olmayan veya kalıcı zararlar verebilirler. Bu sebeple, bu cihazların yeryüzünde radyasyona karşı güvenilirlikleri test edilmelidir. Cihazların test edilmesi uzayda kalacağı süre, konum ve kullanım koşulları gibi birçok faktöre bağlıdır. Test standartları NASA ve ESA gibi uzay ajansları tarafından belirlenmektedir. SPENVIS, ĆREME96 ve ÓMERE gibi yaygın olarak kullanılan bilgi sistemleri veya araçlar, uzay aracının bulunduğu konumun koordinatlarına göre radyasyon ortamını analiz etmek için kullanılır. Tek olay etkisine karşı yapılan kalite testleri ağır iyonlar ile Ulusal INFN Güney Laboratuvarı'nda (LNS) gerçekleştirildi. MAPRad laboratuvarlarında geliştirilen kızılötesi laser sistemi nitel ölçümler için çok yararlı bir araçtır. Birçok cihaz bu laser test düzeneği ile test edildikten sonra iyon testi için LNS laboratuvarlarına alındı. Bu çalışmada, iyon ve laser testi için

kullanılan test düzenekleri detaylı olarak incelendi ve cihazlar iyon demeti ile test edilmeden önce bu test düzeneği GEANT4 ve FLUKA kullanılarak benzetimi yapıldı. Lineer enerji transferi (LET), depo edilen enerji, ve girişim mesafesi gibi parametreler bu similasyon programları sayesinde hesaplandı. Bu similasyonların sonuçları karşılaştırıldı ve değerlendirildi.

Anahtar Kelimeler: Radyasyona dayanıklılık testi, GEANT 4, FLUKA, Lineer enerji transferi

TABLE OF CONTENTS

LIST OF FIGURES

LIST OF TABLES

CHAPTER 1

MOTIVATION

In the present century, space research and avionics have a quiet important place. On the other hand, the production of components and electrical circuits, which are used for scientific research, tactical systems and commercial environment, is either time extensive or financially expensive [1]. The most important thing is the selection of these components for these systems. When the components are chosen for space applications, the important point is the environment of them. It is known that there is a radiation environment because of the galactic cosmic rays, solar flares, electrons and protons in space. The using components or electronic circuits must be radiation hardened in these environments.

Historically, the radiation sensitive components are shielded by some materials to protect at radiation environment [1]. But this method is not accetable because of its cost. The last decades, using of Commerical Of The Shell (COTS) components is popular for space applications because of their low costs. But this components must be tested for radiation environments.

The effects of radiation are Single Event Effects (SEEs), Displacement Damage (DD) and Total Ionizing Dose (TID). These components and electronic circuits should be tested for these effects. These tests have some specifications which are defined by ESA (European Space Agency), NASA (National Aeronautics and Space Administration) or military services [2, 3, 4, 5].

In Europe, the components can be tested at some laboratories with ESA specifications. The most important laboratories for these tests are INFN Catania LNS(Laboratori Nazionali del Sud'), INFN Padova LNL (Laboratori Nazionali Legnaro), Germany GSI, Belgium Catholique de Louvain University Cyclotron

Research Center. These components are exposured to laser and ion beam for SEE phenomena, irradiated with proton or electron beam for displacement damage and irradiated X-ray or ^{60}Co source for test total ionizing dose. Their electrical characteristics are observed during the irradiation. According to these observations, the effects are defined and investigated whether they are permanent or not.

The main purpose of this thesis is to simulate SEE test setup to control the benchmark parameters before the radiation and investigate the laser and ion beam test setup. Chapter2 describes radiation environments, radiation damages, explanation of these damage types and particle interaction with matter and mechanism of occuring events. Chapter3 presents the Monte Carlo simulation packages and explanation of setup simulations. Simulations are made by Monte Carlo simulation packages GEANT4, GRAS, MULASSIS and FLUKA. Chapter4 contains experimental procedure of ion beam test and laser test and results. In Chapter5, simulation and measurement results were compared and discussed.

CHAPTER 2

INTRODUCTION

With developing CMOS technology, the thickness and the size of microelectronic devices and integrated circuits reduce but radiation sensitivity increase. These devices can be exposed to radiation environments because of their application areas [6]. Additionally, high energy physics experiments require them to work under harsh conditions [7].

2.1 Radiation Environments

Space environments are characterized by particles with energies ranging from some keV to several GeV [7]. This particles are categorized by their origin : trapped particles, galactic cosmic rays (GCRs) and solar particles as in Figure 2.1 [8].

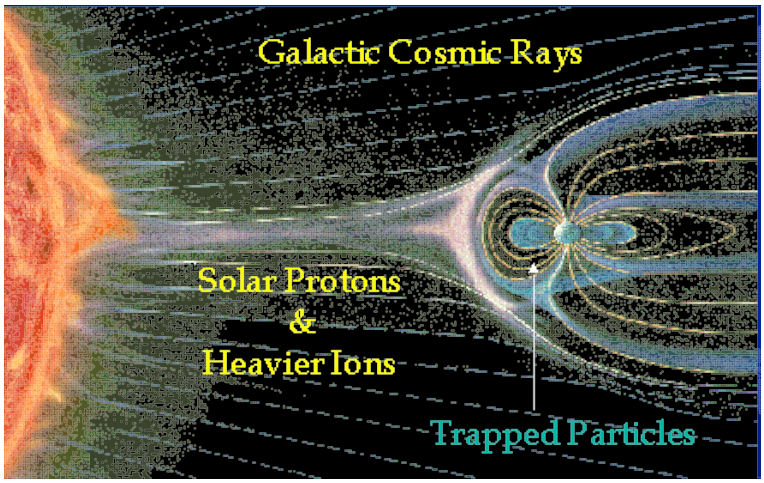

Figure 2.1: Radiation environments and source particles [9].

- **Trapped Particles:** These particles are geomagnetically trapped radiation near the Earth (Van Allen Belts) [8]. Earth has a big magnetic field in space. This huge field creates gigantic magnetic "buble" or geomagnetic cavity. Because of this, electrons whose energies are up to a few MeV and protons whose energies are up to several hundered MeV are trapped in the magnetic field region as shown in Figure 2.2.

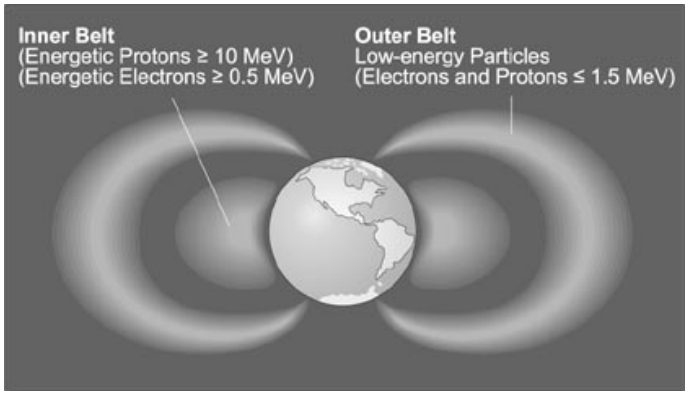

Figure 2.2: Earth Radiation belts or Van Allen Radiation belts [10].

These particles do not reach to atmosphere because the magnetosphere shields these particles [11]. But high energy galactic cosmic rays and solar particles can penetrate the atmosphere. The penetration energy of the particles to the magnetosphere is shown in Figure 2.3 [12].

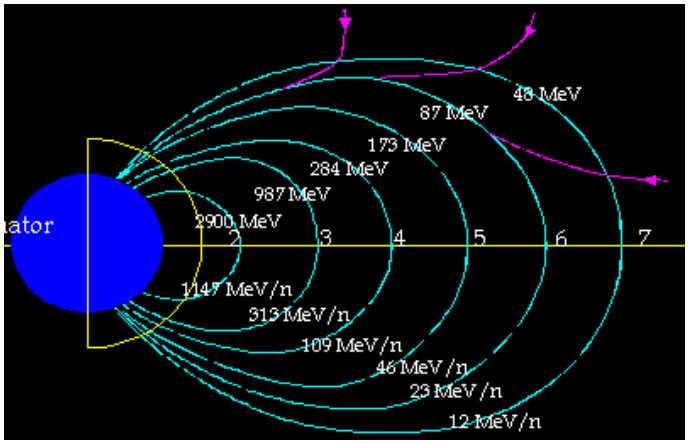

Figure 2.3: Penetration Energies to Magnetosphere [9].

- **Galactic Cosmic Rays (GCRs):** GCRs compose from 85% of protons

14% of alpha particles and remaining 1% includes various ions [6]. The orgin of these rays is remaining out of the our solar system. Although these particles have high energies, they have low flux. When these paritcles interact with matter, their high energies cause ionization effects [13]. CREME and SPENVIS are commonly used simulators to simulate cosmic rays [14, 15].

- **Solar Particles :** The source of these particles is Sun. The unusual bright spot or flares, and solar wind cause to generate solar particles. In nature, the Sun events are not stable. According to some reports [13, 16], solar cycle is divided into two groups solar minimum and solar maximum which takes time 9 and 13 years, respectively.

On the contrary, the important thing to investigate the radiation environments is the coordinate of the space mission such as altitude of orbit, incilanation of orbit. Low Earth Orbit (LEO) is the orbit which approximately 520 km away from the Earth's surfaces [13, 17]. High Elliptical Orbit (HEO) is another orbit. Its low perigee is about 1000 km and high apogee is about 36.000 km [17]. This orbit is effected from solar flares and long exposure galactic cosmic rays [13]. Another type of orbit is Geostationary (GEO) orbits which is the highest orbit. This orbit includes trapped protons whose energies are below the threshold energy of the nuclear reactions.

2.2 Radiation Damages and Mechanisms

In early of 1960, scientists have discovered the effects of radiation at space environments on devices [18]. Space radiation causes some errors and degradation at these devices. Some of these errors are permanent and some of these are soft errors. The mainly occuring damages result from total ionization dose, displacement damage and single event effects. Each effects lead to different mechanisms and different type of damages.

2.2.1 Ionization Effect

Ionization is the process which creates free charges at interacted matter. Also, these free charges can move in material by difussion or drift. α paritcles, protons, electrons or β particles and neutral radiation photons like γ,X rays results in ionization damage. β, α and protons causes direct ionization but X-ray and γ ray cause indirect ionization. For each particle and photons, different physical events can occur. This events will be discussed at the other parts of this chapter.

This particles interact with matter and produce free electrons and holes. Normally, this effect can only give soft errors and effects device performance. In CCDs (Charge Coupled Devices), creation of electron-hole pairs leads to produce dark current and this current effects the device performance [19]. But depending on the system, it can trigger the other damage mechanisms [9].

Additionally, depending on the dose of radiation device performance can change or cause up to failure of the devices. This is called total ionizing dose effects. Total ionizing dose defines the long term ionizing damage due to electrons and protons [9]. In devices, it effects threshold shift, leakage current and fuctional failures.

On the other hand, the amount of energy loss during the ionization is called Linear Energy Transfer (LET) which is unit in $MeV-cm^2/mg$ [13]. The equation is

$$LET = -\left(\frac{1}{\rho}\right)\left(\frac{dE}{dx}\right) \tag{2.1}$$

where dE is radiation energy, ρ is the density of material and dx is the tracking length in the material.

2.2.2 Displacement Damage(DD)

Displacement damage is the another damage mechanism which needs more energy than ionization effect. If the particle creates electron hole pairs, it is called ionizing process [20]. But if sufficiently high energy particles interact with matter, they can move an atom from the lattice side [13]. This event leads to produce vacancies at lattice as shown in Figure 2.4.

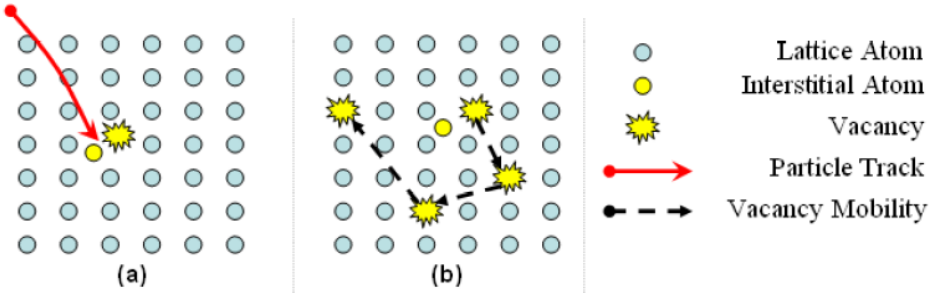

Figure 2.4: Displacement Damage Mechanism a) Particle knocks an atom in its lattice side. b) creation of vacancy [20].

Vacancy is the absence of the atom in regular lattice side. This imperfection in the lattice structure is called a point defect [13]. The placement of this moved atom is called interstitial [13, 20]. The combination of vacancy and intersitial is called commonly I-V pairs or Frankel pairs [12, 13, 20]. This damage results in Current Transfer Ratio (CTR) degradation commonly in optocouplers, solar cells, CCDs, linear bipolar devices. The vacancies can move in lattice at room temperature [12, 20]. So the damage can be treated with annealing methods depending on the devices.

Otherwise, the energy loss during this process defines Non-ionizing Energy Loss (NIEL) [13, 20]. Non-ionizing energy calculation is given by Equation 2.2.

$$NIEL = S_d = \left(\frac{N}{M_2}\right) \Sigma\sigma_i(E) E_r(E) \tag{2.2}$$

where is σ_i is the cross section, E_r (E) is average recoil energy of primary knock atoms, E is energy for an incident particle, N is avagadro's number and

M_2 is gram atomic mass of target [13].

2.2.3 Single Event Effects (SEEs)

Especially, for space applications the other important damage mechanism is Single Event Effects (SEEs) which is related to accumulation of the ionization charged particles [13, 21]. The devices should be tested aganist SEE before they are used in space applications. These tests are usually made by ion beams. There are some important test center in the world. These are listed in ion beam test procedure section of Chapter 4. This event is the special case of ionization. It happens only one particle strikes the strategical place of the contact as shown in Figure 2.5. This event can be classified into three different effects.

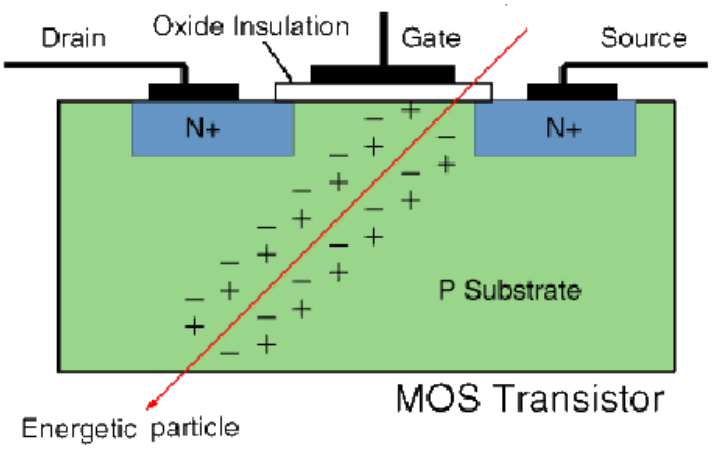

Figure 2.5: Schematically representation of single event effect mechanism [22].

2.2.3.1 Single Event Upset (SEU)

Single Event Upset is defined by National Aerospace Agency (NASA) which reports that "radiation-induced errors in microelectronic circuits caused when charged particles (usually from the radiation belts or from cosmic rays) lose energy by ionizing the medium through which they pass, leaving behind a wake of electron-hole pairs " as it represented in Figure 2.6 schematically. The collection of electron-hole pairs change the logical output of device like change from "0" to

"1" [13]. This causes the soft errors which are not permanent [13, 23]. They can be removed by switching off or reseting the devices [13, 21, 23].

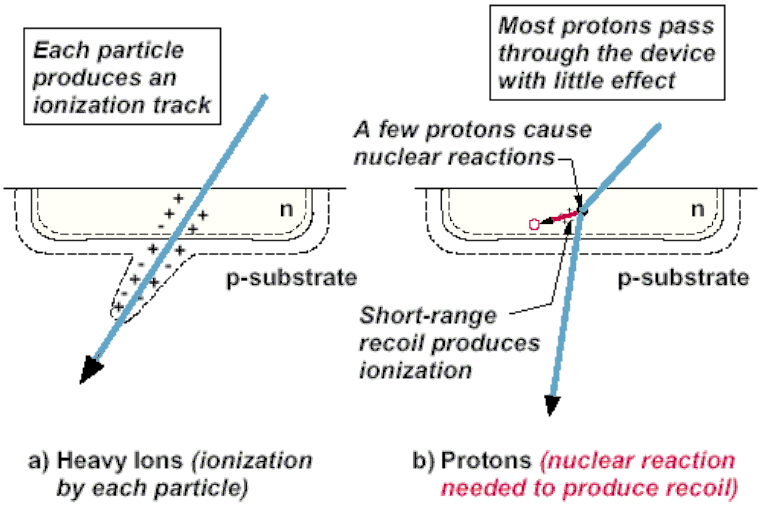

Figure 2.6: Single event upset mechanism for heavy ions and protons [23].

During the ground state tests, heavy ion and proton sources are used to determine the rate of Single Event Upset (SEU). These tests characterize the microelectronic devices respects to SEU [24]. LET vs cross-section graph shows threshold LET for devices as shown in Figure 2.7.

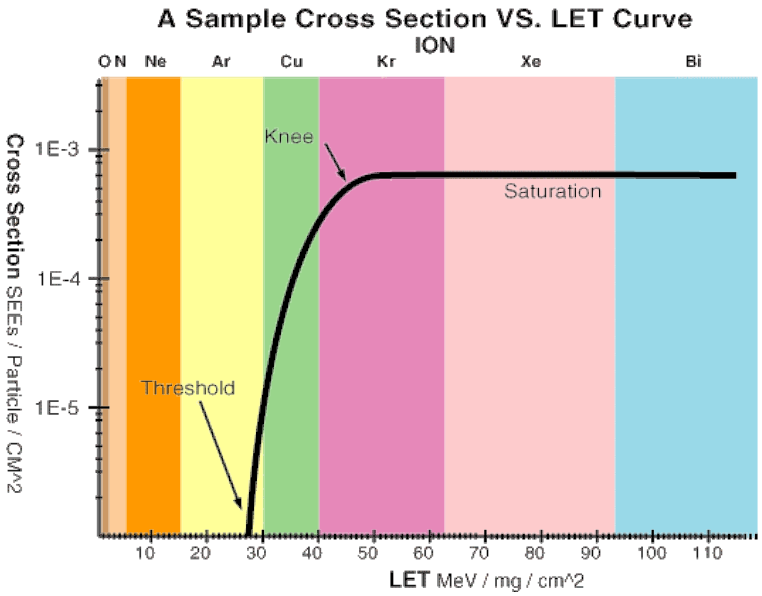

Figure 2.7: A representative LET curve [23, 25].

2.2.3.2 Single Event Latchup (SEL)

Single Event Latchup causes potentially destructive error and may be a permanent damage which is realized by heavy ions, protons and neutrons [13, 23]. SEL was discovered in 1979 by Kolasinski and his co-workers [23] . SEL depends on the temperature because current increases in devices during latchup.

2.2.3.3 Single Event Burnout (SEB)

Single Event Burnout (SEB) leads to a destructive or hard error because of the existence mostly heavy ions, rarely protons and neutrons [23]. Devices like CCDs, power transistors, frozen bits, gate ruptures and some types of linear integrated circuits burn and lose their fuctionality due to SEB [23].

2.3 Particle Through Matter

In this part, interaction of particle with matter which is the most important phenomena of the particle or nuclear physics is explained. It is important because understanding these interactions ensures detection of particle. To detect a particle, it must interact with matter. While particle traverses, it loses energy in material. The amount of energy lost depends on particle type and energy.

2.3.1 Interaction of Heavy Charged Particles with Matter

The common effects are ionization and excitation when the particle passes through the material. If particle has sufficient energy to ionize the matter, the ionization process occurs. However if it does not have sufficient energy, it excites only the electron of atom. These two reactions are the most important energy loss mechanisms.

2.3.1.1 Ionization

Ionization is the most common process for charged particle energy loss. Incoming particle incteracts with atomic electron of nucleus as shown in Figure 2.8. The incoming particle ejects the electron of atom by breaking off the bound of electron. But incoming particle has to have more than the ionization energy of the target bound [26]. During the ionization, incoming particle loses an amount of its energy which equals to the ionization energy of the atom. The result of the ionization, material yields free electrons and positive ions [27, 26]. After the ionization, if the incoming particle has still enough energy, it can repeat this process [28]. In addition, the ionization process is not only valid for charged particle energy loss mechanism but also for electrons and positrons energy loss mechanism.

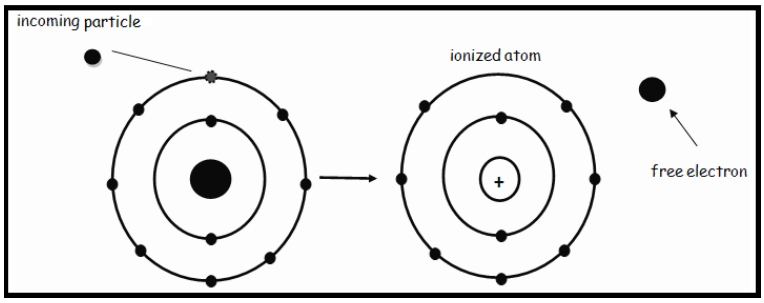

Figure 2.8: Schematical presentation of ionization process.

2.3.1.2 Bethe-Bloch Formula

When the particles interact with matter, they cause some reactions and they lose some or all of their energy. The first energy loss calculation was performed by Niel Bohr [26]. But this formula is not valid for quantum mechanical phenomenon. Because this formula was derivated by classical assumptions [28]. Bethe and Bloch derivated this formula by using quantum mechanical assumptions in 1930. The formula is

$$-\left(\frac{dE}{dx}\right) = 2\pi N_a r_e^2 m_e c^2 \rho \left(\frac{Z}{A}\right)\left(\frac{z^2}{\beta^2}\right)[ln(\left(\frac{2m_e\gamma^2 v^2 W_{max}}{I^2}\right) - 2\beta^2 - \delta - 2\left(\frac{C}{Z}\right)] \tag{2.3}$$

where is N_a is avagadro number, r_e electron radius, I is excitation potential, Z is atomic number of absorber, A is atomic weight of absorber, ρ is density of absorber, z is incident particle charge in units of e, $\beta = \nu/c$ of incident particle, γ^2=$1/(\sqrt{1-\beta^2})$, δ is density correction, C is shell correction, and finally W_{max} is maximum energy transfer in a single collision.
Moreover, $2\pi N_a r_e^2 m_e c^2 = 0.1434 MeV cm^2/g$. Although Bethe-Bloch equation includes quantum mechanical assumptions, it has also limitations. These are;

i.) Velocity limitation ; Bethe-Bloch formula is inversely depend on β. If velocity of particle increases more than 0.96c, this formula is not valid [26, 27, 29].

ii.) Channeling effect; when a particle goes through the crystal with critical angle, it generates channel-like way to travel with a minimum scattering. This phenomenan is called chanelling effect [29]. Thus it loses its energy during this motion. This energy loss can not be calculated with Bethe-Bloch formula since the amount of energy is very small [27, 28].

On the other hand, this formula includes density correction and shell correction. Density correction is used at high velocities and shell correction is used at low velocities. Main reason of density correction is medium polarization. If the particle electric field is bigger than medium electric field [28], the medium reduces the electric field of particle because of medium polarization [28]. Density correction term is defined by δ and this value can be found by using Sternheimer's parametrizations [28, 30]. The second correction is shell correction. It is applied when the incoming particle velocity is not bigger than the velocity of electron in

which states at the orbital of the atom [28, 31]. The second correction term is $2C/Z$ as in Equation 2.3 [28]. In addition to this, formula is really accurate for low velocity particles because of β^{-2} term [32].

2.3.2 Interaction of Electrons and Positrons with Matter

The occuring process depends on the energy and velocity of electron when an electron or positron passes through the matter. Their energy loss process is different from those of the charged particles because of their high velocity and small masses [26]. Electrons and positrons lose their energy in two ways which are scattering or collision and radiaiton, when passing through the matter [27]. Collision types are Moller Scattering, Bhabha Scattering and ionization [27, 28, 26]. Radiational types are Bremsstrahlung, Čerenkov, transition and annihilation. The events are explained in detail at the following parts.

On the other hand, Bethe-Bloch formula is modified to calculate the energy loss of electrons or positrons [26, 27]. The resason of this modification is to distinguish an incoming particle from a target particle because both are electrons [27]. Bethe-Bloch formula is generally given by Equation 2.3 by using Equation 2.4 for electrons,

$$-\left(\frac{dE}{dx}\right) = 2\pi N_a r_e^2 m_e c^2 \rho \left(\frac{Z}{A}\right)\left(\frac{1}{\beta^2}\right) ln[\left(\frac{m^e \beta^2 c^2 \gamma^2 T}{2I^2}\right) + F(\gamma) - \delta - 2Z/C] \tag{2.4}$$

where T is the kinetic of particle and $W_{max} = \frac{T}{2}$, the other constants are the same with the original formula [27]. Another difference between first formula and the second formula is $1/\beta^2$ term. At the first equation, this term includes z/β^2 but at second equation incident particle charge unit is ignored.

2.3.2.1 Bremsstrahlung

One important energy loss mechanism is Bremsstrahlung which emanates interaction between an incoming electron and the nucleus of atom [27, 31, 32]. The incoming electrons declerate because of the nuclues. Then it loses some of energy and produce radiation. This special type of radiation is called Bremsstrahlung radiation [26, 32]. The process is shown as in Figure 2.9. The energy of this radiation is equal to difference between initial energy and final energy of the incoming electron [31].

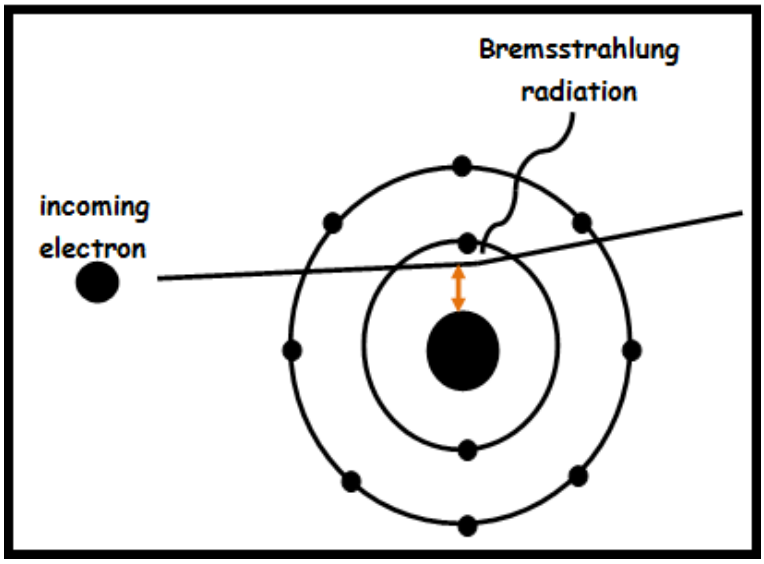

Figure 2.9: Schematical presentation of Bremsstrahlung radiation.

2.3.2.2 Čerenkov Radiation and Transition Radiation

When an electron or another charged particle traverse from one medium to another medium, which has different refraction index, radiation is emitted which is called transition radiation [30]. Čerenkov radiation is another energy loss mechanism for electrons. The mechanism is similar to Bremsstrahlung radiation but for Čerenkov radiation, incoming electron must change medium and velocity of the incoming electron must be bigger than the velocity of light in that medium [26]. Basically, the presentation of this process is shown in Figure 2.10. But both

of these radiational energy loss mechanisms use at high energies [30].

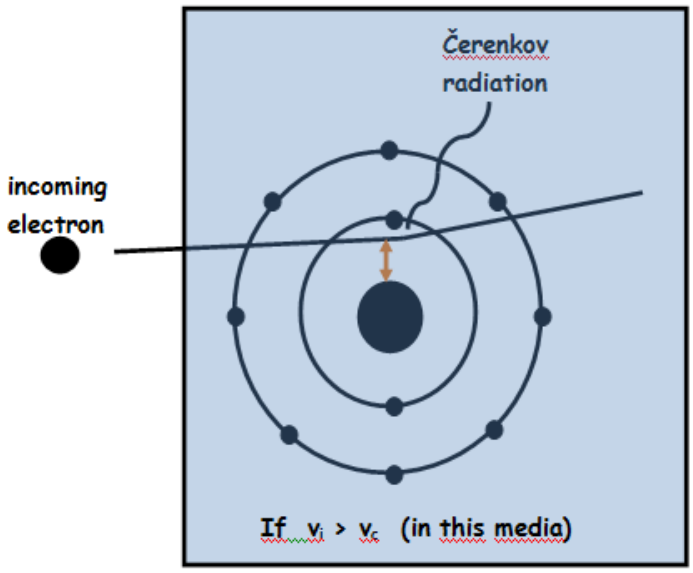

Figure 2.10: Schematical presentation of Čerenkov radiation.

2.3.2.3 Electron-Positron Annihilation

This process is satisfied for high energies and conserved laws. When an electron and a positron collide with each other, they emit gamma rays [30]. These gamma rays have high energy. This collision is called electron-positron annihilation as in Figure 2.11.

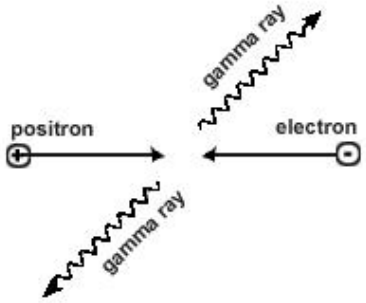

Figure 2.11: Electron-Positron Annihilation [30].

After the collision of electron and proton, they emit radiation and the electrical charge, momentum, and total energy are conserved.

$$e^- + e^+ \rightarrow \gamma + \gamma \tag{2.5}$$

We know that electrons and positrons do not lose their energy with radiative way. They lose their energy with collisional ways which are Moller scattering and Bhabha scattering. Schematically, representation of these scattering mechanisms is shown in Figure 2.12 [32].

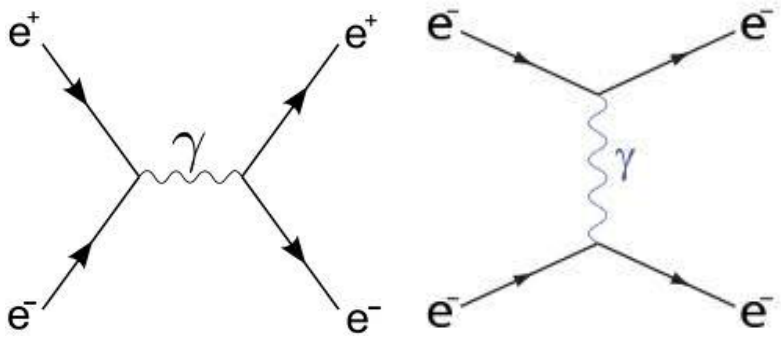

a) Mollerscattering. *b) Bhabhascattering.*

Figure 2.12: Special cases of electron-positron annihilation.

2.3.2.4 Critical Energy

When a particle interacts with matter, it loses its energy by two ways, collisional and radiative. For a particle, when the amount of radiative energy loss is equal to the amount of collisional energy loss, this energy value is called critical energy loss [26, 27, 28].

2.3.2.5 Radiation Length

Radiation length is an important parameter for the radiative energy loss of electron and charged particles. It gives distance where the particle starts radiative energy loss or where it starts to emit radition such as Bremsstrahlung [26, 27, 31]. This parameter is reduced by $1/e$ factor [26]. It describes as Equation 2.6.

$$E = E_0 e^{\left(\frac{-x}{L_{rad}}\right)} \tag{2.6}$$

In this equation E_0 is initial energy, E is loss energy and L_{rad} is radiation length(cm), x is the thickness of material [27]. According to this formula radiation length depends on initial energy of particle and thickness of the material. There is another approximations to calculate this value. This approximation is given in Equation 2.7 [26].

$$X_0 = \left(\frac{716.4A}{Z(Z+1)ln(287\sqrt{Z})}\right) \tag{2.7}$$

In that equation X_0 is radiation length whose unit is (g/cm^2), Z is atomic number, A is the atomic mass of the target material.

2.3.3 Interaction of Photons with Matter

At previous parts, the interaction of particles with matter was explained. When particles pass through the matter, two main processes occur; ionization and excitation. But photons do not ionize when they interact with matter. Photons cause interactions in variety of ways with respect to energy range of photons. The photons lose their energy with photoelectric effect, compton scattering and pair production, additionally, Rayleigh and Mie processes. The most well-known interactions are photoelectric effect, compton scattering and pair production. These interactions depend on energy of photon and atomic number of the matter as in Figure 2.13.

2.3.3.1 Photoelectric Effect

This process was completely discovered by Einstein and he won the Nobel Prize [26]. A photon, which has sufficently enough energy, can emit an atomic electron from a material [26, 32]. As a result, photon energy is absorbed by electron and the electron releases [26, 34, 32]. Photons energy is defined as

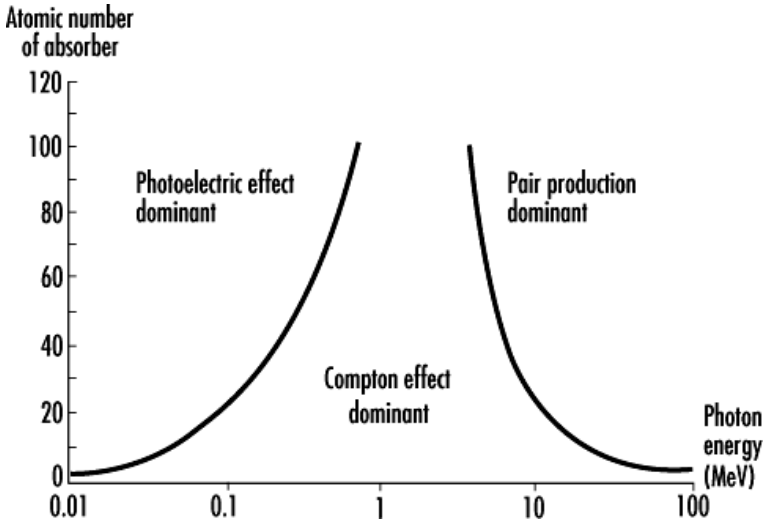

Figure 2.13: Relation between photon energy and atomic number of matter [13].

$$E_\gamma = \frac{h}{\gamma} = \frac{hc}{\lambda} \tag{2.8}$$

The delivered energy of photon must be greater than binding energy of target material. For metals this energy is called work function and represented as ϕ [26]. If the photon energy is larger than the work function, the rest of the energy is carried away by the emitted electron as Equation 2.9 [26];

$$E_e = E_\gamma - \phi \tag{2.9}$$

where E_e is emitted electron energy, E_γ is photon energy and ϕ is work function. This process can be observed in free atoms. Photon is absorbed by an atom and atom becomes unstable. Electron of atom from higher level fills the gap to return to stable situation [26, 32]. The process is shown as in Figure 2.14.

2.3.3.2 Compton Scattering

Compton scattering is a process which represents inelastic scattering of photons to free or loosely bound electrons. These electrons are at rest. Historically, Compton scattering was recognized by Compton in 1923 [26, 33]. During the ex-

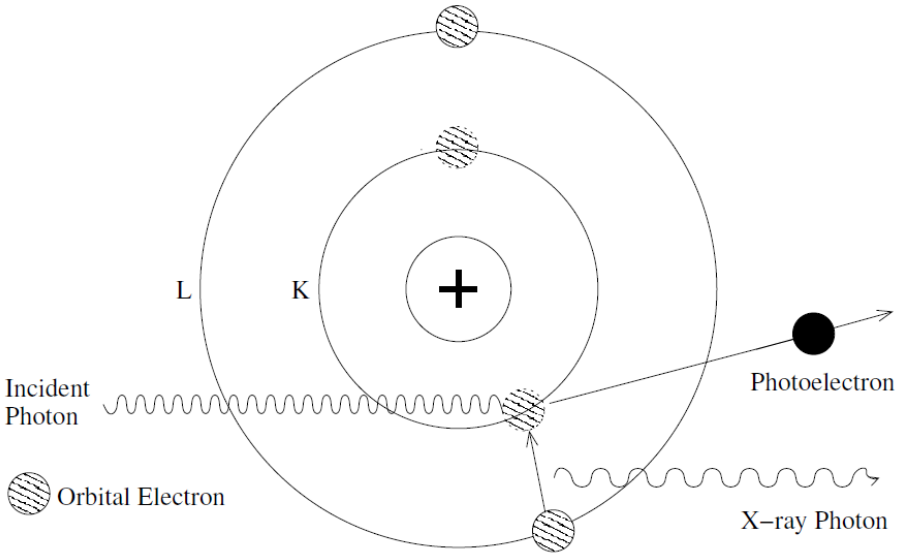

Figure 2.14: Description of photoelectric effect in free atom [26].

periments he realized that the incident photon wavelength and scattered photon wavelength were different [26].

For bound electrons, Compton scattering is more likely than photoelectric effect when the electron energy is sufficiently high [26, 32]. Compton scattering formula is derived by using fundamental energy and linear momentum conservation. The formula is;

$$\lambda = \lambda_0 + \frac{h}{m_0 c}[1 - cos\theta] \tag{2.10}$$

In this formula λ is wavelength of outgoing photon and λ_0 is wavelength of incoming photon and θ is angle between incident and outgoing photons [26]. The representation of Compton scattering is as in Figure 2.15.

2.3.3.3 Pair Production

Pair production is a high energy phenomenan. However, photoelectric effect and Compton scattering are low-energy and mid-energy phenomenan, respectively [27]. A photon must have an energy which is greater than 1.022 MeV to occur pair production [32]. This process occurs between a high energy photon

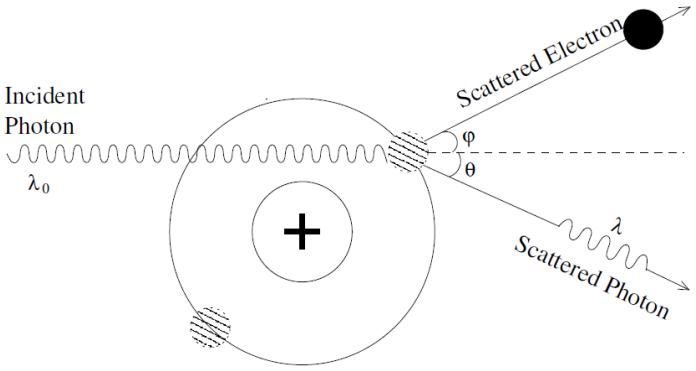

Figure 2.15: Compton scattering of a photon [26].

and a nucleus. Incoming photon interacts with Coloumb field of nucleus and as a result of this, energy of photon converts into a pair (electron-positron) [27, 32, 34]. The process can be explain by;

$$\gamma + X \rightarrow e + e^{+} + X^{*} \tag{2.11}$$

where X and X^{*} represent ground and excited state of a nucleus, respectively [26]. Pair production is a dominant mechanism for high energy photons especially $\gamma - ray$ interaction at sufficiently high energies [34].

2.3.4 Multiple Scattering

Multiple scattering is the scattering of charged particle at several times, statistically more than 20 scatterings [29]. The multiple Coloumb scattering is theorized well by Moliere whose theory describes the angular distribution of scattering roughly Gaussian for small angles but at larger angles it behaves like Rutherford scattering [28]. The problem is to calculate the net angle of deflection as a function of thickness of target material [27]. Calculation of multiple scattering includes really complicated steps and formulations.

To calculate the multiple scattering, instead of considering total deflection, it is convenient to consider its projection in a plane [27, 28]. On Gaussian approximation, rms(root mean square) value is projected plane for small deflection

angles as [28];

$$\theta_0 = \theta_{rms}^{plane} = \sqrt{\frac{1}{2}}\theta_{space}^{rms} \tag{2.12}$$

After this, according to Gaussian approximation for small angles, the angle distribution is; [28, 34]

$$\theta_0 = \frac{13.6MeV}{}z\sqrt{\frac{x}{X_0}}[1 + 0.0038ln(\frac{x}{X_0})] \tag{2.13}$$

Besides Moliere, the calculation of multiple Coloumb scattering is studied by Goudsmit - Sounderson. But these two theories give only angular distribution. On the other side Lewis theory computes the moments of spatial distribution [27, 28, 34, 35].

2.3.5 Interaction of Neutral Particles with Matter

Neutral particles mean that electrically neutral. Neutrons are similar with protons in terms of having the same mass, nucleon number and spin [32]. In contrast to this, they do not interact with Coloumb forces in terms of this behaviour like photons [27, 26].

Low-energy neutrons generally interact *inelastically* [26]. Result of this inelastic scattering leaves the target nucleus in an excited state. The reaction occurs as this formulation [26].

$$n + X_p^{n+p} \rightarrow n + [X_p^{n+p}]^* \tag{2.14}$$

The excited nucleus becomes unstable and emits a neutron of lower kinetic energy [26].

Elastically scattered neutrons can transfer their kinetic energy to nuclear centers [32]. This occurs recoiling and provides signals (e.g ionization). This signals reveal the presence of the neutrons [26]. In this process, after the collision,

the target nuclues remains the same state [26]. It is not excited. The reaction is [26]

$$n + X_p^{n+p} \rightarrow n + X_p^{n+p} \tag{2.15}$$

2.3.5.1 Fission

Fission is one of the most important reaction which a neutron can initiate [26]. This process occurs between a slow neutron and a heavy nucleus [26]. Neutron is captured by heavy nucleus and heavy nucleus state change to an excited state. After, fragmentations occur with a brief delay [26]. During this process, several neutrons and γ-ray are emitted from the nucleus. For example, Uranium fission is written as; [26, 32]

$$n + U_{92}^{235} \rightarrow I_{39}^{139} + Y_{53}^{95} + 2n + \gamma \tag{2.16}$$

The end of the reaction iodine and yttrium are commonly products.

2.3.5.2 Spallation

Another process, which includes neutron interaction, is spallation. If energy of neutron is greater than 100 MeV, spallation becomes important [26]. When a high energy neutron interacts with a nucleus, the nucleus fragments into several parts and this is called as spallation [26].

2.3.5.3 Transmutation

In this process when neutron reacts with an element, it changes the element into another element [26]. Transmutation occur in all energy range of neutron [26]. An example of this reaction is

$$n + B_5^{10} \rightarrow Li_3^7 + \alpha \tag{2.17}$$

In this reaction, Boron is captured by neutron. Boron-10 is converted into Lithium-7 and it emits α-particle.

CHAPTER 3

EXPERIMENTAL PROCEDURE

Two type of tests which are ion beam test and laser test, are performed to investigate the performation of the electronic circuits or/and DUTs under radiation environments. Firstly, laser test was performed in MAPRad Laboratory, at Perugia. After data were evaluated by the DUTs or/and electronic circuit's company or/and manufacturers, ion beam test was performed in Catania, LNS (Laboratoria Nazionali del Sud'). The test procedure of this two method is described above in detail.

3.1 Laser Test

Firstly, DUTs are tested with laser. Laser test is like a pre-test before ion beams. Because it is not as realible as ion beam test but it shows the general errors about DUTs.

3.1.1 Laser Test Benchmark

Equipments:

- Laser Model: ML20A15
- Lenses

  LA1027, LB1676-B, LC2679-B, LA1608-B, LB1945-B, LD2297, LA1131-B, LB1409-B
- Polarizer (Melles Griot)
- Beam Splitter and Cube Beam Splitter Holder (Newport CH♯1)

- Objectives 100X (MITUTOYO B47051901)
- CCD Camera(1/3â ccd image sensor CB2818-B)
- Dual Timer(C.A.E.N Mod. N938)
- NIM-TTL-NIM Adapter(C.A.E.N Mod. 89)
- Oscilloscope
- Photodiode (Newport model:818-RB-40), Load 50 ohm

Experimental test setup of the laser is not complex but the important thing for this setup is to focus laser on the DUT. The way of calculation of the energy deposition on DUT surface and evaluation on effects on these device depend on the laser focalization. The components are placed as in Figure 3.1.

As in Figure 3.2, the laser passes firstly from the polarizer and reaches beam splitter which splits the laser beam into two side. Some amount of laser, which is about 5% of the total beam, goes through the DUT surface. The other part of the beam, which is about 40% of the total beam, goes to CCD (Charge Couple Devices) camera left side. The beam, which is gone to the DUT surface, passes through the some lenses and optical zoom devices before reach the DUT surface.

The other beam, which is gone to the CCD camera, pass some lenses, too, before reaching the camera. On the other hand, when the first beam (its percentage is 60) reaches the DUT surface, some of the beam are reflected from there and again pass from the beam splitter and finally it reaches the CCD camera. This provides monitoring the DUT surface. Because monitoring the surface make the focalization of the beam easier. This results in accurate calculation of energy deposition and evaluation of the events like Single Event Upset (SEU), Single Event Latchup (SEL).

On the other hand, the energy of laser can be changed during the radiation. Photodiode is used to calculate the laser energy. The laser signal is observed by

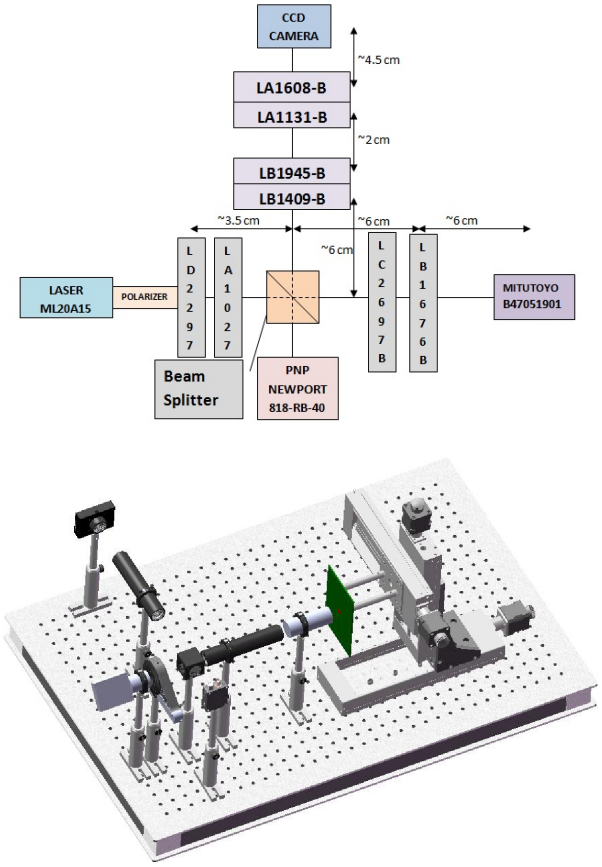

Figure 3.1: Schematically the bench system on top and bench at bottom designed with Solidwork.

oscilloscope as shown in Figure 3.3.

Formula of the energy is defined as

$$E = 10^{-9} \left(\frac{P_{area}}{l_c \times R_p} \right) \times S_{cc} \tag{3.1}$$

where P_{area} is area of the triangle at the photodiode laser signal, the signal is as in Figure 3.3, l_c is load resistance with 50 ohm for this photodiode, R_p is sensitivity of photodiode, which is 0.5 A/W, $S_{cc} = (1 - reflectedbeam)$ is absorbtion capability of silicon. S_{cc} means that amount of absorbed beam by photodiode because some amount of beam reflected from photodiode. This calculated energy is equal to the surface kinetic energy at DUT. So, using this energy value, Linear Energy Transfer LET can be calculated easily. The formula of the Linear Energy

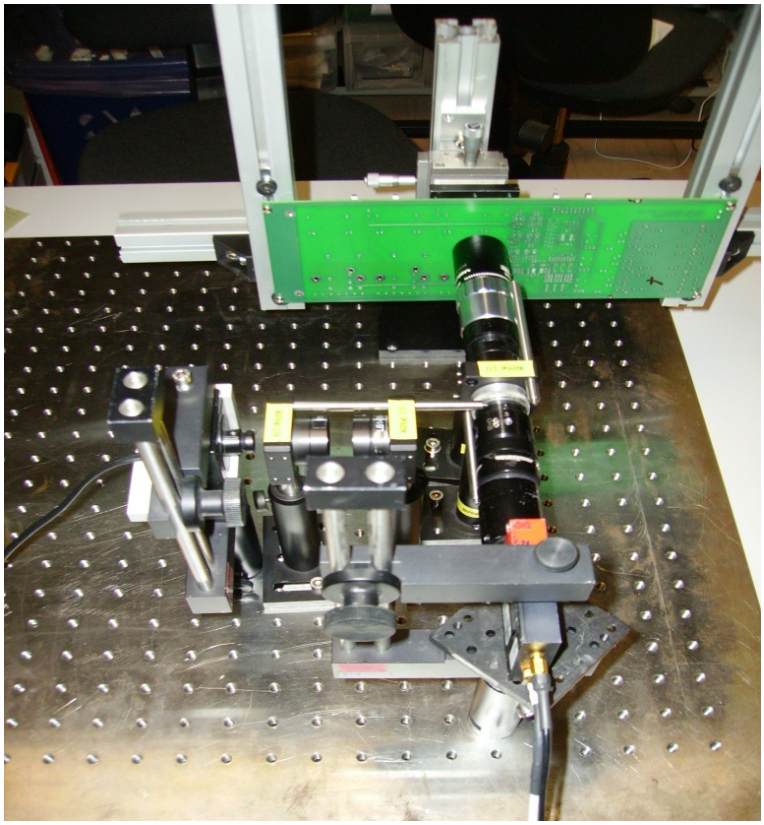

Figure 3.2: Picture of setup with all components.

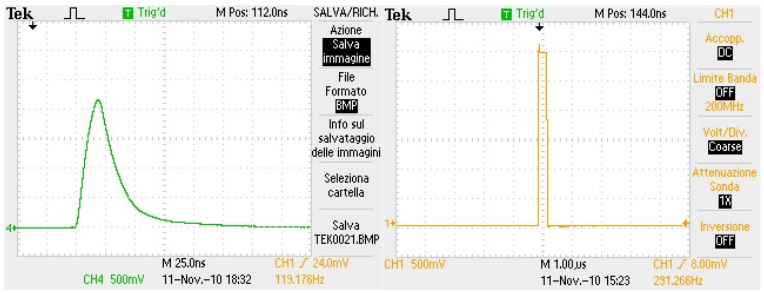

Figure 3.3: Laser signal.

Transfer LET is defined as [36]

$$LET = \left(\frac{E}{\rho_{Si} d_{Si}}\right) \tag{3.2}$$

where ρ_{Si} is the density of silicon or any using material, d_{Si} is the penetration depth of the silicon. In Table 3.1, it includes the calculation of energy and LET.

The DUT is radiated with laser by scaning along horizontally and vertically. During the radiation process changing parameters of DUT and occuring events

Base	Tall	Area	Energy	Energy (eV)	Energy (MeV)	LET
62	21	65.1	$4.48966\ 10^{-09}$	$2.8060\ 10^{10}$	$2.8060\ 10^{04}$	150.5383
nsec	V	ns V	J	eV	MeV	$MeV/mg/cm^2$

Table 3.1: Example of energy calculation of laser signal

like SEU and SEL were controlled simultaneously.

3.2 Ion Beam Test at LNS (Laboratoria Nazionali del Sud) in Catania

We know that developing CMOS technology requires some disadvantages besides advantages. As the devices getting smaller and thinner, they become more sensitive to radiation. So they have to be tested in order to be used under radiation environments. At ground level, the most realible test is ion beam test to investigate whether the devices are hardened to radiation or not. There are some different test laboratories which have different test facilities. The list of this laboratories is as below.

- Single Event Effects Testing Services, Canada
  $http://www.re-labs.com/$
- Sandia National Lab, CEA/DIF, France
  $http://www.sandia.gov/about/index.html$
- Lawrence Berkeley Labs 88" Cyclotron (LBL - heavy ion)
  $http://user88.lbl.gov/home$
- NASA/GSFC Radiation Effects & Analysis
  $http://radhome.gsfc.nasa.gov/top.htm$
- Boeing Radiation Effects Laboratory (BREL)
  $http://www.boeing.com/assocproducts/radiationlab/services.htm$

- Brookhaven National Laboratory(BNL) SEUTF
  $http://tvdg10.phy.bnl.gov/$
- U.S Naval Research Laboratory, $http://www.nrl.navy.mil/$
- Texas A & M University(TAMU) Cyclotron (heavy ion)
  $http://cyclotron.tamu.edu/ref/$
- Michigan State University National Superconducting Cyclotron Laboratory, (MSU NSCL)
  $http://www.nscl.msu.edu/$
- Crocker Nuclear Laboratory(CNL), University Of California
  $http://crocker.ucdavis.edu/Site/Research/RadiationEffects.aspx$
- The Svedborg Laboratory Radiation Testing Services (SEE), Sweden
  $http://www.tsl.uu.se/welcome.html$
- ESA-ESTEC Californium-252 Assessment of Single-event Effects CASE (ECIF member)
  $https://escies.org/ReadArticle?docId=227$
- National Space Development Agency of Japan (NASDA)
  $http://www.jaxa.jp/index_e.html$
- Center of Space Science and Applied Research , Chinese Academy of Sciences
  $http://english.cssar.cas.cn/l/dse/SEELab/$
- Canada's National Laboratory for Particle and Nuclear Physics, Tri-University Meson Factory (TRIUMF)
  $http://www.triumf.ca/headlines/current-events/$
  $triumf-hosts-cisco-systems-week-long-for-testing-period$

- Paul Scherrer Institute(PSI), Switzerland
  $http://www.psi.ch/psi-home$
- Indiana University Cyclotron Facility (IUCF)
  $http://www.iucf.indiana.edu/$
- Argonne National Laboratory ATLAS
  $http://www.phy.anl.gov/index.html$
- Helmholtz Centre for Heavy Ion Research GmbH(GSI), Germany
  $http://www.gsi.de/$
- Grand AccÃ©lÃ©rateur National d'Ions Lourds(GANIL), (National Large Heavy Ion Accelerator), France
  $http://www.ganil-spiral2.eu$
  $/ganillab/presentation?set_language=en$
- Istituto Nazionale di Fisica Nucleare (INFN) Catania, Italy
  $http://www.lns.infn.it/$
- Istituto Nazionale di Fisica Nucleare (INFN) National Labratory of Legnaro, Padova
  $http://sirad.pd.infn.it/sirad/WEB/Index.htm$
- Oslo Cyclotron Laboratory, Norway
  $http://www.mn.uio.no/fysikk/english/research/about/infrastructure$
  $/OCL/index.html$
- Radiation Effects Facility RADEF at the University of JyvÃskylÃ Finland (ECIF member)
  $https://www.jyu.fi/fysiikka/en/research$

These laboratories are the accelerator laboratories. In addition to this, there are some companies to product the test system. MAPRad is the one of these

companies which design the test system with the innovative ideas in Perugia, Italy.

The ion beam test which is aganist the SEE, was performed according to ESA specifications [2]. Same specifications about general and test plan for our test setup are;

- The radition field should be placed over the area of device ± 10% [2].
- The silicon thickness should be at least 30 μm and flux range should be from 100 $ions/cm^2/s$ to 10^5 ions/cm$^2/s$ on the DUT [2].
- Irradiation can be performed in air for heavy ions but devices should be shileded from incident light [2].
- About 5 exposures should be required to adequately plot LET vs cross-section curve [2].
- When devices is irradiates at an angle, an effective LET shall be calculated as the normal incidence LET divided by cosine of the angle as in Equation 3.3 [2].

$$LET(effective) = LETcos(\theta) \tag{3.3}$$

In Catania, the used test system was designed by the MAPRad. The setup equipments are scintillator, silicon strip detector, DUT holder, three motors for moving the DUTs and silicon strip detector, shutter . The purpose of all these equipments are explained respectively as following;

- **Scintillator:** The main reason of the using scintillator is to count the coming particles and to measure particle flux and fluence from beam pipe. The scintillator is connected the photomultiplier tube (pmt) and it connects NIM crate. It contains NIM-TTL-NIM adapter, dual timer, gate. By using these modules, the particles, which impinge on the scintillator, can be controled

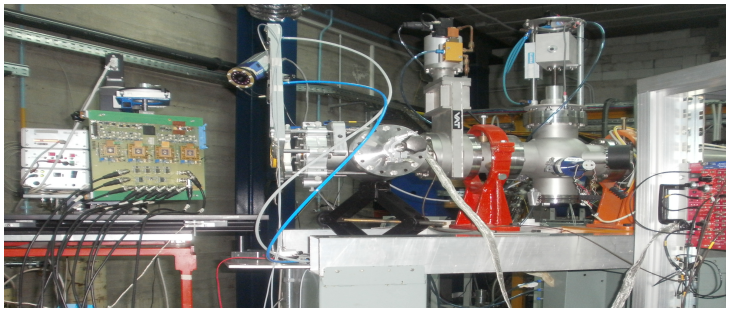

Figure 3.4: SEE test setup in LNS.

with software. So this provides to measure the beam fluence prior the test starting. Additionally, changes at the fluence is observed simultaneously.

- **Silicon Strip Detector:** The particles coming from the beam pipe are passed through firstly kapton, secondly scintillator, and finally silicon strip detector. Silicon strip detector is placed near the DUT holder. The function of silicon detector is to analyze the beam profile, before the DUT irradition. The beam profile is investigated by using a program code written in ROOT software [37] which gives the energy of charge distribution at the surface of the detector. According to this beam profile, DUTs are placed the beam profile.

- **Motors for Motion:** The set up motion is managed with three motors which are contolled by Labview program [38]. This ensures that the placement of DUTs along beam axis is done accurately before the irradiation is started.

- **Shutter :** The aim of shutter is to stop beam particles urgently since it takes some time. The beam flux generally does not have an expected value at the first time. So we need to wait to reach to an expected fluence. During this time, the shutter is turned off not to effect the DUTs /circuit or silicon detector. When the fluence reaches expected value, shutter is turned on to check beam profile or irradiate the DUTs.

Test setup is as in Figure 3.4 with all components. Before the irradition, the position of the DUTs is adjusted by using a laser. The laser is used for measuring the distance. The laser is connected to the system as in Figure 3.5.

Figure 3.5: Control the system with laser.

The motors, which move the DUTs holder and silicon strip detector can be controlled by LABVIEW program of which the front panel is shown as in Figure 3.6. At this front panel, the direction buttons provide holder's movement by using laser.

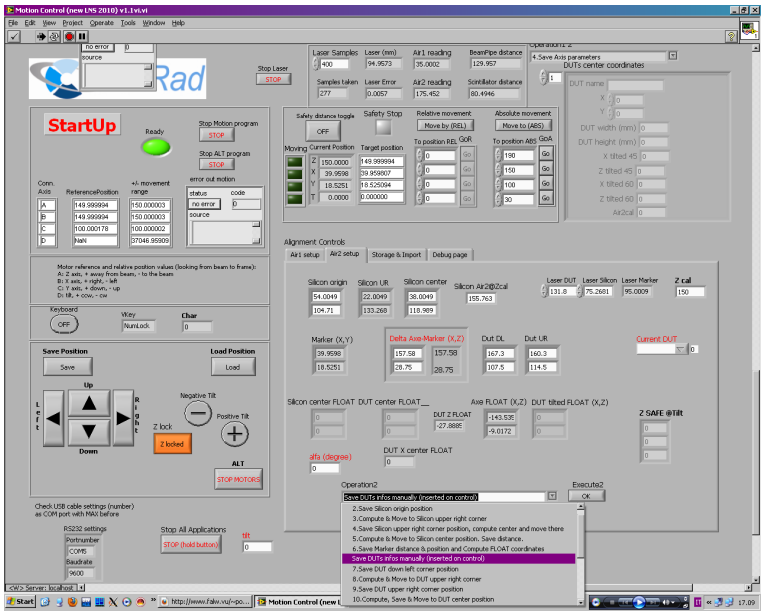

Figure 3.6: Front panel of Labview.

The second important thing is to check beam profile before starting the irradiation. The main purpose of the beam profile check is to place the DUT inside the

beam area correctly. So the DUT is not directly irradiated, firstly checking the beam area. Beam comes to silicon strip detector. Then the charge distribution graph is drawn by using the ROOT as in Figure 3.7.

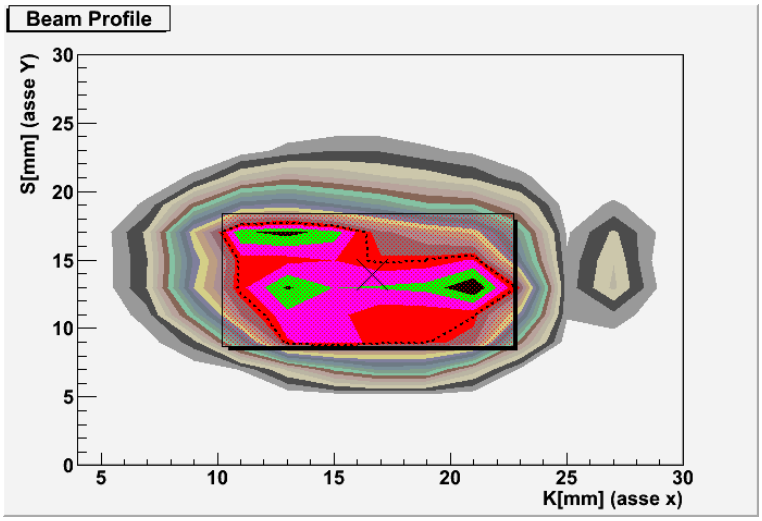

Figure 3.7: Beam profile of Xenon ions.

After the beam is checked and DUTs are taken place inside the beam profile, everything is ready for starting the irradiation. This position is showed as in Figure 3.8. The integrated DUTs/circuit is operated, before the radiation and outputs are recorded by manufacturer of the DUTs/circuit. After they prepare for the operating like usual, the radiation is started. During the irradiation, the outputs are compared with the recorded outputs and this process continues until the DUTs/circuit is finished in one cycle. It depends on the fluence of beam. It sometime takes twenty minutes or fifty minutes or even more. DUTs/circuits are irradiated with different ion beams which have different energy and frequencies. For this test, used ion beams are ^{20}Ne,^{40}Ar,^{84}Kr,^{129}Xe. During the irradiation, the system can be observed outside the radiation area by a camera. If there is unsual or wrong thing during the irradiation, firstly shutter is closed to protect the DUTs/circuits, secondly beam is closed because shutting down the beam takes some minutes. After this when the beam area is safety to enter inside, it is possible to go inside and fix the problem or change something about the setup

or DUTs/circuits.

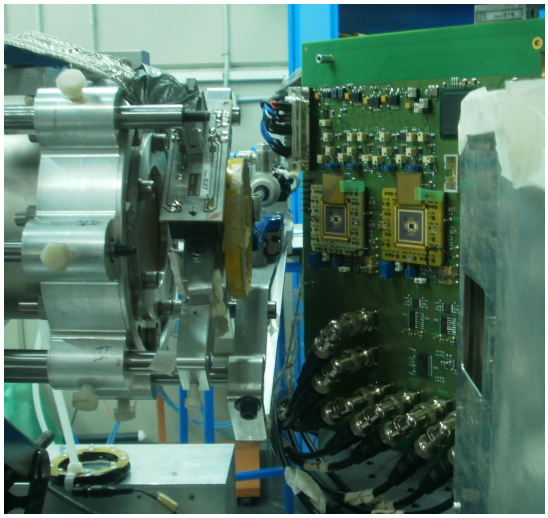

Figure 3.8: Position of DUTs before irradiation.

These tests are operated at room temperature about 18-22 Â°C. On the other hand, another option increases the temperature with a heater gun while testing. The temprature of the DUTs can be increased up to 200Â°C-500Â°C. Because this is useful way to investigate SEEs which are based on the increasing temperature of the DUTs/circuit. Additionally, each step of the test is abided by the ESA (European Space Agency) specifications which is ESA/SCC Basic Specifications No:25100: Single Event Effects Test Method and Guidelines. Before the test to project LET and tracking length in the silicon GEANT4 simulation was used. According to simulation, the radition test table as in Table 3.2.

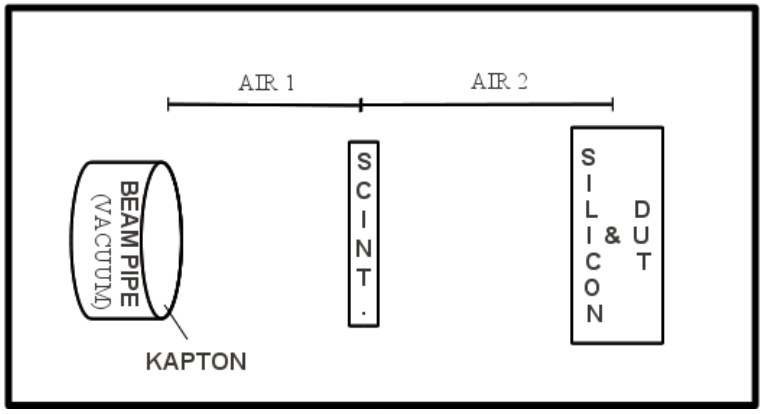

Figure 3.9: Schematic representation of ion beam test setup.

Ion Type	Air 1 (cm)	Air 2 (cm)	Kapton Thickness(μm)	Scintillator Thikness (cm)	Angle (deg)	LET (MeV/mg/cm^2)	Range (μm)
^{20}Ne	5	20	50	100	0	2.64	255
^{20}Ne	5	20	50	100	60	5.28	127
^{40}Ar	5	20	50	100	0	10.2	101
^{84}Kr	5	10	50	100	0	33.1	68
^{84}Kr	5	7	50	100	0	36.3	50
^{129}Xe	5	10	50	50	0	60.7	51
^{129}Xe	5	10	50	50	45	85.8	36

Table 3.2: Ion beam test irradiation table.

Schematic representation of the setup is shown as in Figure 3.9 to understand some variables at the setup.

CHAPTER 4

SIMULATIONS OF ION BEAM TEST SETUP

4.1 SIMULATION OF SETUP WITH GEANT4 (GEometry ANd Tracking 4)

GEANT4 is the most commonly used simulation toolkit which is based on C++ programming language. The application areas of this simulation tool is wide such as nuclear physics, high energy physics, medical applications, accelerator physics and space physics. So, it provides more sensitive and optional simulation. In this project, GEANT4.9.3.p02 is used. The simulation of Single Event Effect (SEE) test setup starts with geometry description and material definition (detectorconsturction.cc), after it requires description of physics which includes types of particle and physics models (physicslist.cc). It finishes with the definition of events which includes the calculated parameter you need(Run Action.cc and SteppingAction.cc) . These are obligated sources fundamentally. But additionally, visualization of geometry and process, more physics output, trajectories can be defined.

Description of Geometry: The setup includes three layers which are kapton, scintillator and silicon. The test was realized at air. So the world material was described as air at "DeterctorConstruction.cc" file. The setup was placed in that world and X,Y,Z coordinate system is initialized. Each layers were described as solid, logical, physical which mean the shape of the volume, material of the volume and position of the volume respectively. Kapton layer is a tube whose radius is 2 cm and thickness is 50 μm. Scintillator and silicon layer are box whose thickness are 100 μm and 1.5 cm respectively. When the layer was positioned,

the origin of the layer was defined as midpoint of their volume. The distance between kapton tube and scintillator box is called Air 1 which is equal to 5 cm for all mesurements. Air 2 is the distance between scintillator box and silicon box. This distance is 20 cm for Ne, Ar ions, and 10 cm for Kr and Xe ions, 7 cm for Kr ion at only one measurement. This parameters were shown at Table 3.2 in previous chapter. Changes about the thickness of layers and other parameters are made by macro file which provides to run the program interactively as in Figure 4.1.

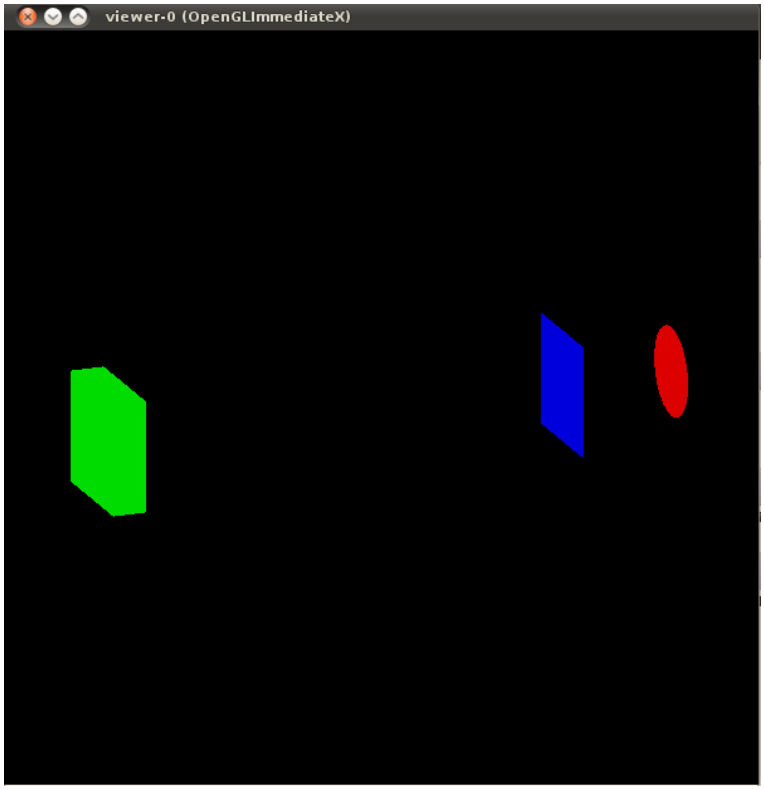

Figure 4.1: Geometry of setup.

Description of Physics list: After the description of geometry, the most important thing is the description of physics list. Because GEANT4 does not have a default physics list. Mainly, two physics processes ,which are electromagnetic and hadronic, exist in GEANT4. But these physics process are divided into subgroups like low energy em, high energy em or low energy neutron physics, ion physics, radioactive decay. The setup physics list includes standart elecromagnetic physics

and all possible events are classified by the particles. Bremsstrahlung, ionization and multiple scattering are defined for electrons. Additionally, for positrons, e-e+ annihilation was included. Gammas are associated with photoelectric effect, coloumb scattering and gamma conversion. For protons and muons, multiple scattering, ionisation, bremsstrahlung and pair production are defined seperately as in Figure 4.2. Otherwise cut values are adjusted 10.0 μm as default.

Additionally, for ionization, there are several types of calculations with respect to different particles. The valid interfaces are G4eIonization, G4eBremsstrahlung, G4hIonisation, G4ionIonisation, G4ionGasIonisation, G4mplIonisation, G4MuIonisation, G4MuBremsstrahlung, G4ePolarizedBremsstrahlung, G4ePolarizedIonisation.

G4eIonisation: This process calculates the maximum energy transfer like as below. It looks like Bethe-Bloch formula but it is modified by M.J Berger and S.M Seltzer. So, it is called Berger-Seltzer formula;

$$\left(\frac{dE}{dx}\right) = 2\pi r_e^2 mc^2 n_{el} \left(\frac{1}{\beta^2}\right) \left[ln\left(\frac{2(\gamma+1)}{(I/mc^2)^2}\right) + F^{\pm}_{(\tau,\tau_{up})} - \delta\right] \tag{4.1}$$

where n_{el} is electron density in material, r_e is classic electron radius, mc^2 is equal to mass energy of electron, I is mean excitation energy in the material, $\beta^2 = 1 - 1/\gamma^2$, T_{cut} is minimum energy cut for γ -ray production, δ is density effect correction, $\tau = \gamma - 1$, τ_{up} is min(τ_c,τ_{max}).

G4eBremsstrahlung: This process is a part of the GeVEnergyLoss and this includes bremsstrahlung radiation by the electrons and positrons. G4hIonisation is used to calculate energy loss with ionisation by hadrons (π+, π-, K+, K-, σ+, σ-, anti-proton, anti-sigma+, xi-, xi+, He^3, α and generic ion). The other interface includes the other options about the energy loss by ionisation.

Description of Events: This step contains that the definition of stepping action and run action. For this project, the calculation of energy deposition (Edep), tracking length and linear energy transfer (LET Silicon) at silicon were pointed step by step at source file "SteppingAction.cc". For each particle, energy

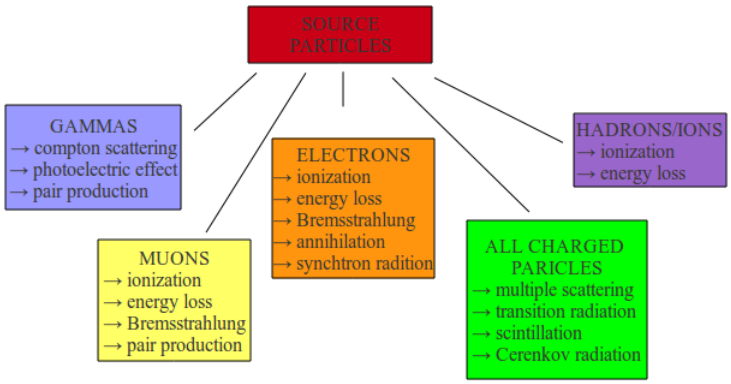

Figure 4.2: Schematic representation of physical events respect to source particles at em scenario.

is 20 MeV/n. RunAction.cc file specifies the start and end of the run. It creates histograms, tuples with root files at the beginning of the run and then at the end of the run writes the all outputs to the root extension file.

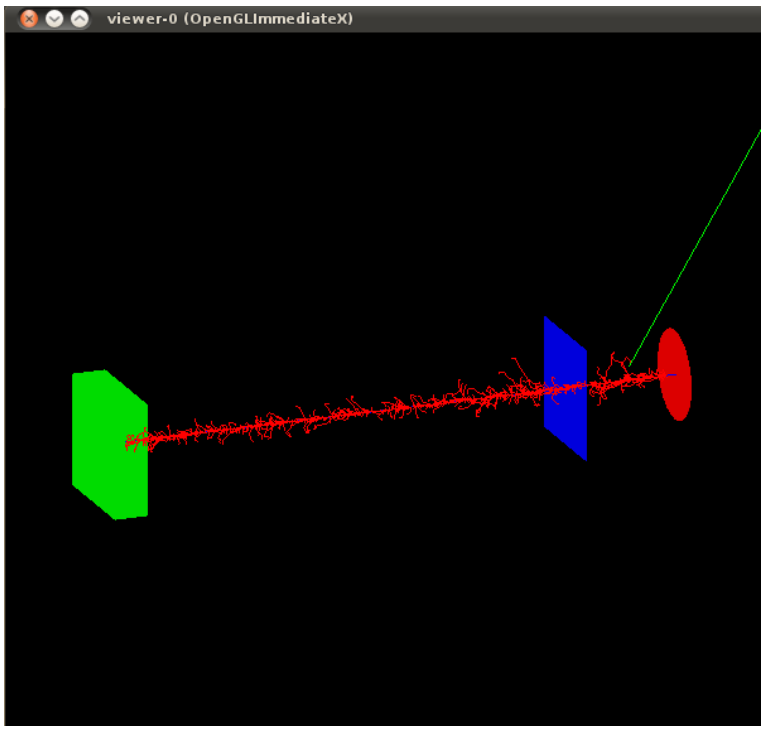

Figure 4.3: Runing GEANT4 for Ne ion.

Visualization: GEANT4 includes seven visualization drivers which are OpenGL, OpenInventor, HepRep/WIRED, DAWN, VRML, RayTracer, ASCIITree. In Figure 4.3 OpenGL was used for visualization. These wide range visualization op-

tions provides to observe geometries, which are even more complex, with tracking, zoom and rotation options.

End of the Run: During the run, deposited energy for each layers, linear energy transfer at the silicon and track length at each layers were outputed at screen for each of beams. After the running, the average value of these outputs were printed at screen and root file was created which includes graph of these outputs.

4.2 SIMULATION OF SETUP WITH MULASSIS (MULti LAyer Shielding SImulation Software)

Radiation shielding is an important process for electronic circuits and/or DUTs which are used in radiation environments. There are some tools and softwares to analyze it. One of these softwares is MULASSIS, which is GEANT4 based, easy to use and commonly used software. This GEANT4 tool can be used with SPENVIS interface or can be installed locally. This software provides construction of 1D planary and spherical geometry, analysis options like particle attenuation, radiation ionizing dose, non-ionizing dose and energy deposition [39]. But it doesn't provide the LET (Linear Energy Transfer) so, LET was calculated from the formula,

$$LET = -\left(\frac{1}{\rho}\right)\left(\frac{dE}{dx}\right) \tag{4.2}$$

where ρ is the density of target material, dE is the surface kinetic energy of the material, dx is track length in the material. So it can be defined as energy loss per unit length. MULASSIS gives the energy loss information and track length information after the run. But this LET calculation is not very accurate.

Mainly, this program is used to investigate the energetic particles interaction with matter. By using this program can be produced one-dimensional geometry and analysis of dose, NIEL (non-ionizing energy loss), tracking length and fluence. When it is analysised these values, it uses different calculation parameters or formulations. These formulations depends on the choosen physics scenarios. Physics scenarios are categorized into types of particles and energy range of particle.

There are four different types physics scenarios with different calculations which are standard em (electromagnetic) physics, hadronic physics, low neutron (ln) physics and binary. In addition to this, combinations of this scenarios can be used according to project.

In this project, the suitable physics scenario is “hadron+em-ln” for our setup. It means that hadronic particle transport with ionisation and standard lepton-gamma transport, but it does not include low-energy neutron.

St-em (standard electromagnetic process) energy range is 1 keV to 10 PeV [40, 35]. At “leem” (low energy electromagnetic process), energy range is from 250 eV to 1keV for electrons and gammas [42]. For hadronic process, the energy range starts about 1 MeV and goes up to 15TeV [41]. The haronic process contains 19 MeV neutron cutoff energy but this value is lower than 19 MeV for low-energy neutrons [40]. Binary cascade is inside the hadronic process but energy range is about from 10 MeV to 10 GeV.

At the end of the run, output file, whose extention is .rpt, include the deposited energy each layer, tracking length and the other output file is .cvs which contains fluence analysis data. Additionally, .eps file is created for visualitization of the layers as in Figure 4.4.

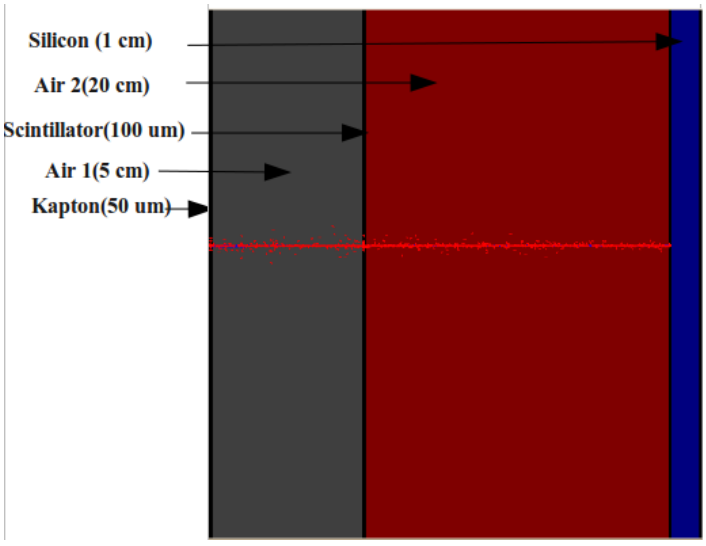

Figure 4.4: Vizualization of the setup layers.

4.3 GRAS (Geant4 Radiation Analysis for Space)

GRAS is another simulation tool which is based on GEANT4. This software specifies a framework to coordinate development of GEANT4-based applications for space radiation analysis. It allows 3D geometry with GDML and C++, some analysis types like dose, fluence, NIEL, energy deposition and total ionizing dose (TID) and different physics scenarios and histogramming outputs with ROOT and AIDA. The most important differences between MULASSIS and GRAS for our project are that GRAS provides 3D geometry definition and LET (MeV/cm) calculation at silicon layer. LET is calculated by G4EM calcutor and using dE/dx table. Because of these reasons, GRAS supplies more accurate calculations than MULASSIS. Geometry of the setup is shown as in the Figure 4.5 which is 3D .gdml file. The .gdml file was opened by GraXML.

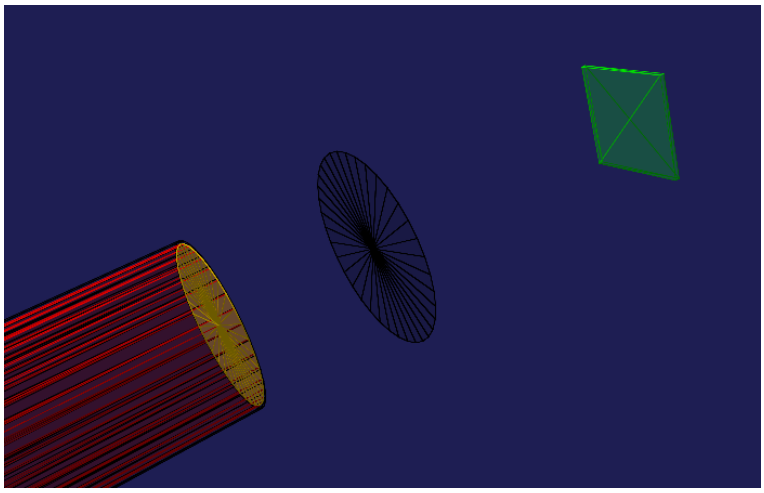

Figure 4.5: 3D set up geometry with GraXML.

At the end of the run, .root , .cvs, .out files were taken. ROOT file is a tree which includes track length, deposited energy at each layer, LET at silicon layer graphically. Fluence analysis exists in the .cvs. All events during the run are contained step by step inside the .out file and end of the file all calculated variables, which are total average dose (MeV), LET value (MeV/cm) and track length(μm), are printed.

4.4 FLUKA

FLUKA is the another Monte Carlo simulation package. This simulation package can be used areas like radiotherapy, accelerator driven system, particle physics etc. But main goal of FLUKA is to simulate the particle interaction with matter and particle transport [43]. FLUKA includes an input card whose extension is .inp and format is ASCII. This file has some command lines which contain six floating point values (they are called WHATs) and one character string (called SDUM) [43].

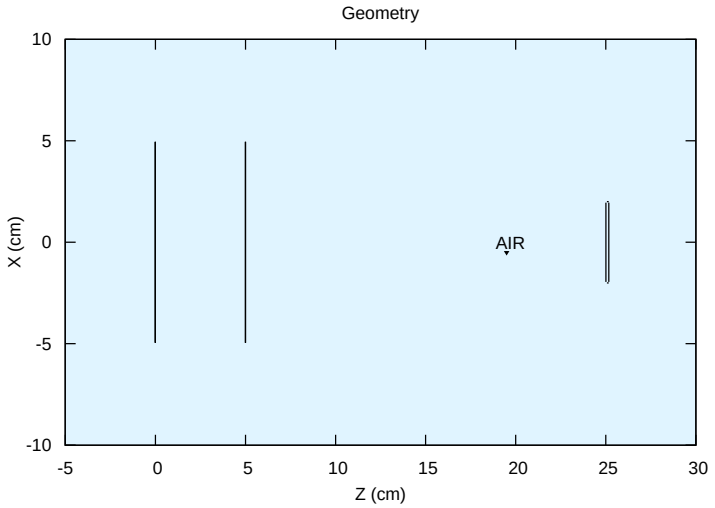

Figure 4.6: Geometry of test setup with Fluka.

At the same time, FLUKA has an interface the lines are created automatically. It appoints some number or strings respect to chosen option from the interface. All parameters about the simulation are defined by this way. After the definition of parameters like geometry definition, particle definition, calculation type, the important thing is to choose the analysis type which is called estimators.

In our project, defaults part which means that calculation type of the simulation was arranged PRECISIO. After that, the most important part is the definition of the geometry. The set up geometry includes blackbody region, void,

world region, kapton region, scintillator and silicon region. Blackbody is whole body of the set up and dimension is 1000x1000x1000 cm. Black body region is defined as "+blckbdy -void". It means that the area composes extraction of void from the whole body. Void is defined as a box whose dimension is 30x30x60 cm. World region composes extraction of the kapton layer, scintillator layer and silicon layer from void. The other regions like kapton region, scintillator region and silicon region contain kapton layer whose shape is RCC (Right Circular Cylinder) and thickness is 500 μm and radius 5 cm, scintillator layer whose shape and radius are the the same with kapton layer but thickness is 100 μm Silicon layer dimension is 4x7x1.5 cm, and its shape is RPP (Rectangular Parallelpiped).

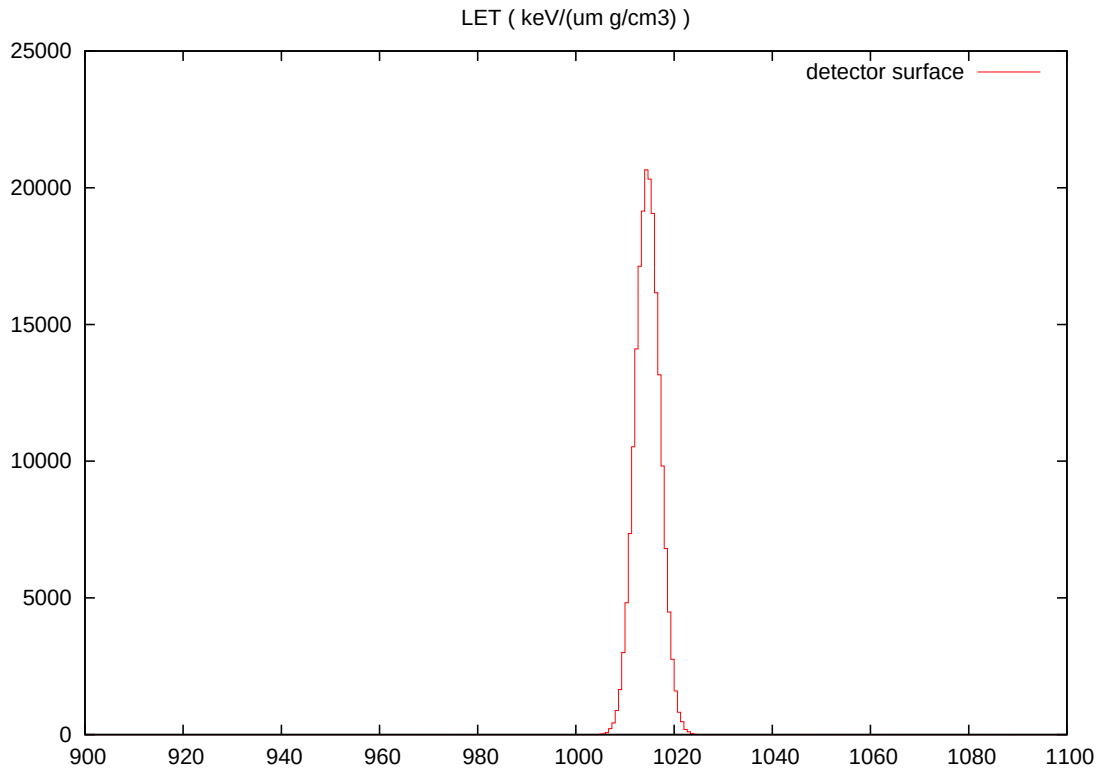

Figure 4.7: LET distribution graph with FLUKA by using USRYIELD estimator.

The other important part is the definition of estimators. Estimators identify the types of output file. USRDBX, USRBIN, USRYIELD and USRTRACK estimators are used for fluence analysis, distirubution of energy at the geometry, LET at silicon and tracking length of beam at silicon detectors respectively. Output

graphs for USRYIELD and USRBIN are as in Figure 4.7 and Figure 4.8.

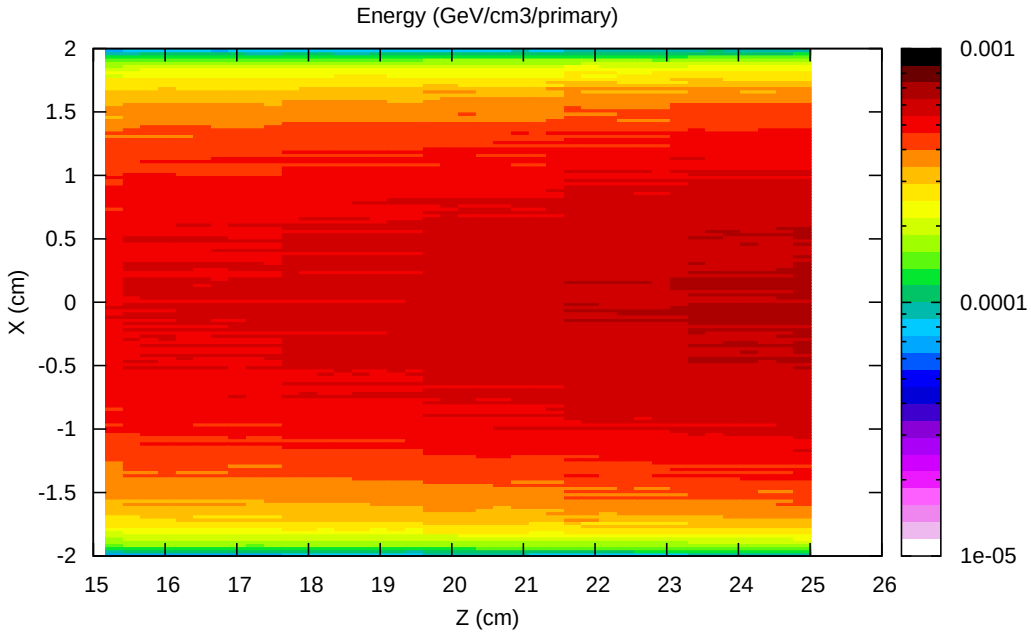

Figure 4.8: Beam profile at silicon along the X-Z axis.

CHAPTER 5

SUMMARY AND RESULTS

This work contains investigation and explanation of Single Event Effect (SEE) test setup details, some calculation and measurements before and during the tests. Our team works on development of ion beam test setup (Catania site) and laser test setup.

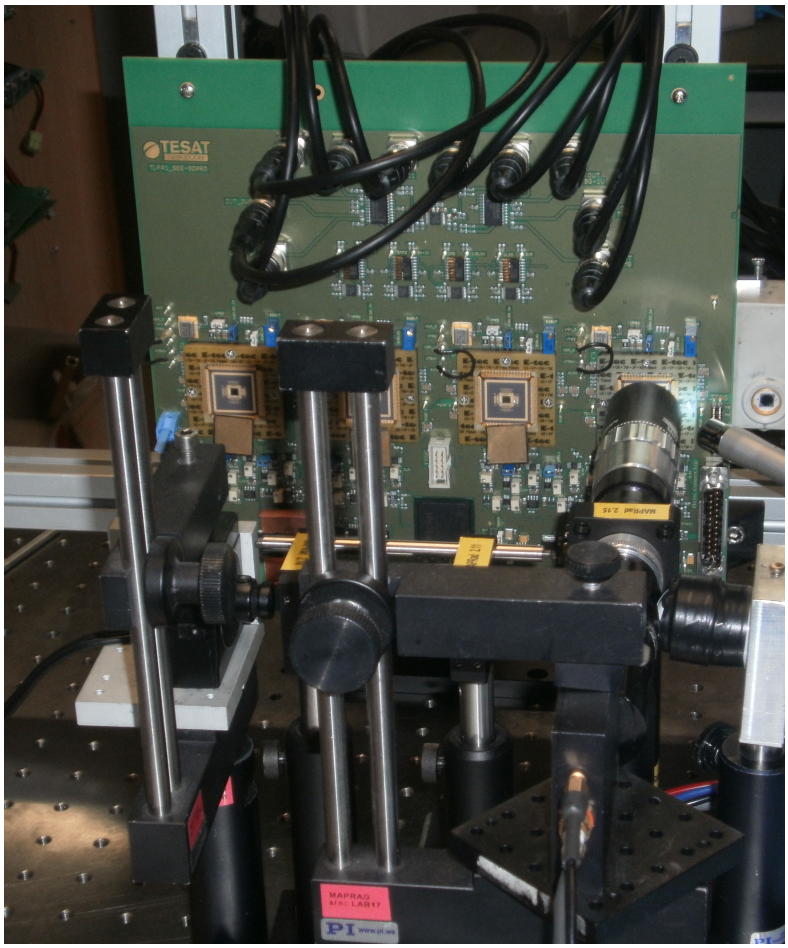

Figure 5.1: Laser test setup during irradiation the DUTs.

Backside laser test is the first step of SEE test. The laser system is used for qualitative measurements. An infrared pulsed laser system was developed in

MAPRAD laboratories. Several devices were tested at infrared laser beam setup then were taken to Catania, LNS laboratory for testing with ion beams. This laser setup capability is SEE studies of electronic components by simulating heavy ions. According to simulated LET values, energy of laser is adjusted and the DUTs are irradiated. Energy of laser adjustment and calculation were explained in Chapter 3. Figure 5.1 shows laser test setup during the irradiation of devices. There were exactly same four DUTs. These devices started to be tested, seperately. During the test, laser was focused on the DUT surface and DUT was scanned sensitively with laser. A great amount of SEUs were recorded at digital part of this device when scanning it. But suddenly, a SEL was observed at analog part of this device during the irradiation. After this, device manufacturers wanted to stop irradiation. Because SEL can fail the system when the device use in a system. Due to this, manufacturers took their devices to prevent SEL and they revised structure of the devices.

The second step is heavy ion beam test in Catania. In Europe there are limited number of accelator sites which are delivered ion beams fulfill the requirements of ESCC standards for SEE testing. Four selected ion beams can be used for testing ^{20}Ne,^{40}Ar,^{84}Kr,^{129}Xe. This test is performed to qualify the device aganist SEE after laser test. DUTs, which were controled aganist SEL after laser test, were ready to irradiate with ion beams. Before irraditon, beam profile was checked with double sided silicon detector (SiGesPes). According to this beam profile, DUTs were placed inside this beam area. Each DUTs, which are four and exactly the same, were irradiated with ion beams as in Chapter 3 Table 3.2. The reason of the irradiation of the same DUTs is to increase the results statistically. During the irradiation of devices, when atomic number of ion beam is increased, number of SEU increased, too and during Xe ion irradiation, SEL was observed again. At the end of the ion beam test, it was noted that devices were not radiation hardened.

The main purpose of ion beam test is to calculate LET values and count SEUs in unit area (cm^2) respect to calculated LET values as in Figure 5.2. The important thing is to chose correct LET values for drawing this graph. As explained before in Chapter 2, at single event effect section, the graph is composed by three part; threshold, knee and saturation. For each parts, at least three LET values should be imported to fit Weibull distribution.Because Weibull distribution is a mathematical description of the failure behavior in a population of identical components. So this distribution has been found to be a reasonable model for describing device failures due to single particles [44]. The Weibull distribution defines LET versus cross-section graph as a function of four parameters as in Equation 5.1 [44].

$$\sigma(L) = \sigma_{sat}(1 - exp[-((L - L_0)/W)^s)] \tag{5.1}$$

where σ_{sat} is asymptotic saturation cross-section (cm^2), L_0 absolute LET threshold ($MeV - cm^2/mg$), W is statistical width ($MeV - cm^2/mg$) and s is statistical shape.

Otherwise, SEUs are counted by measuring voltage change due to ionization or accumulation of charge at the DUTs during the irradition. To change the â0â into â1â or vice versa, the voltage difference $\triangle V$ must be around 1.5 V [34].

In that graph LET values were calculated by GEANT4. LET is calculated by Equation 5.2.

$$LET = \left(-\frac{1}{\rho}\right)\left(\frac{dE}{dx}\right) \tag{5.2}$$

where dE is energy (MeV), dx is particle track length(um) in material and ρ is density of material (g/cm^3). The detector material is silicon so ρ is 2.321 g/cm^3. dE and dx values were recorded from simulation and charge measurement. From the charge measurements, simulated energy data relability was calculated. The

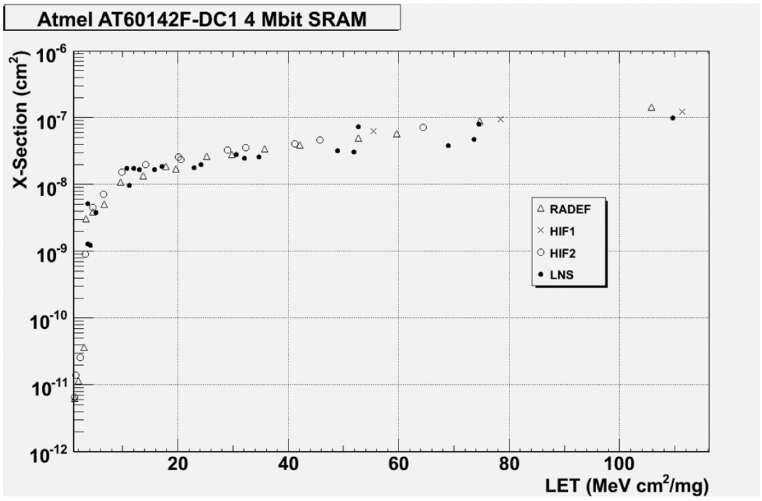

Figure 5.2: LET versus cross section graph [45].

calculation was explained step by step;

1. Charges were collected by Double Sided Silicon Detector (SiGesPes) during irradiation. For Ar ions, charge graphs are as in Figure 5.3. Each graphs were fitted with gauss function. These fits give mean and rms values.

2. The rms and mean values of graphs with and without gaussian fit, and most probable values were recorded.

3. Surface kinetic energy, track length and LET values were recorded by two different Monte Carlo simulations. Details about the GEANT4 and FLUKA were mentioned in Chapter 4.

4. Figure 5.4 shows most probable charge versus surface kinetic energy. Kinectic energy values were recorded by GEANT4 and FLUKA as in Table 5.1. These graphs were fitted with a polynominal function, named *pol*1, in ROOT [37]. Equation of these fits are $y = 0.00716x - 517.9$ and $y = 0.106x - 969.5$ for GEANT4 and FLUKA, respectively. Then by using mean charge values from gaussian fits, surface kinetic energy values were calculated with equations as in Table 5.2.

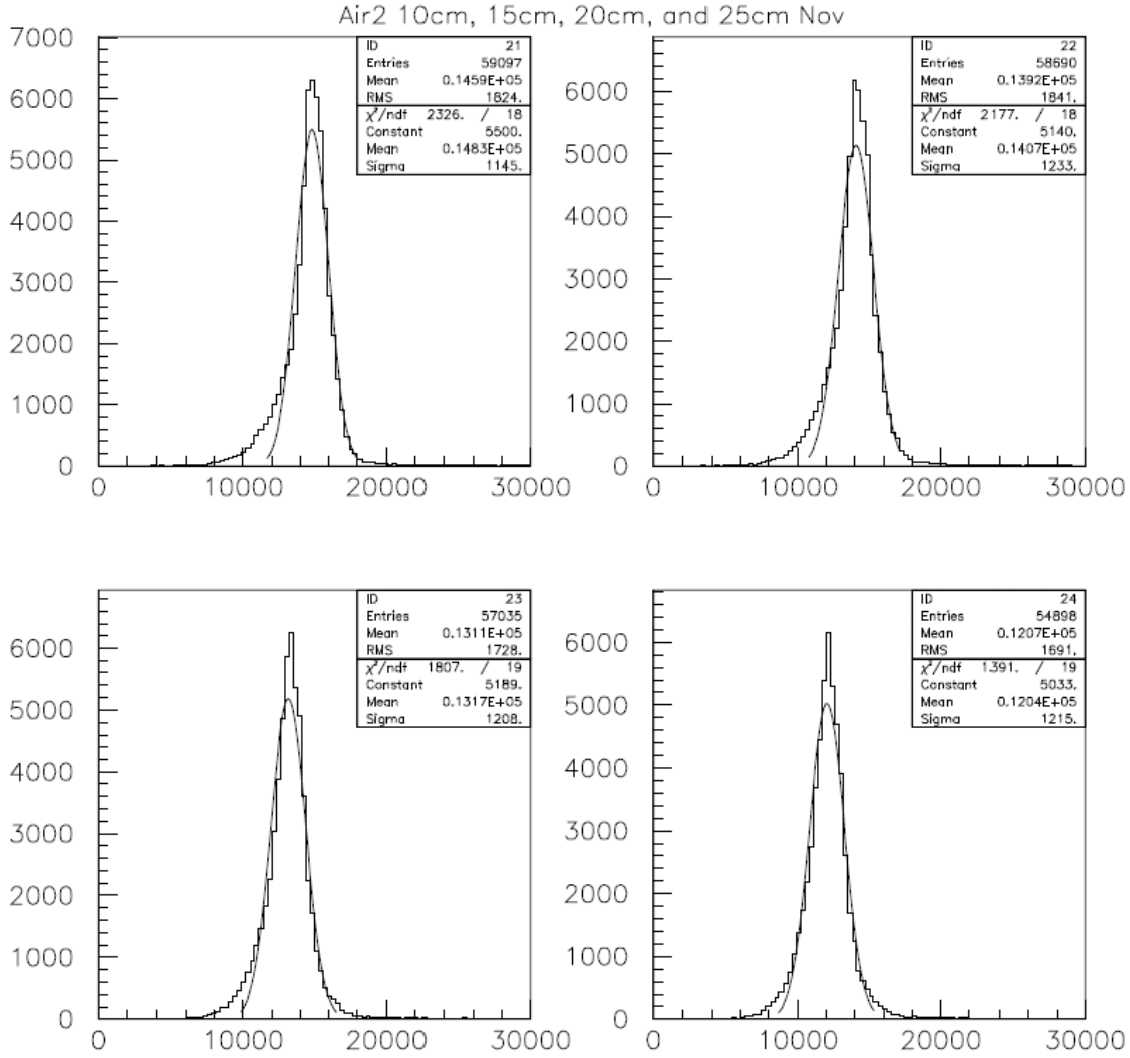

Figure 5.3: Charge graphs for Ar ions with different Air 2 values. Air 1 was fixed as 5 cm. But Air 2 changes 10 cm, 15 cm, 20 cm, 25 cm respectively.

Ion Type	Air 2 (cm)	S.K.Energy(MeV)FLUKA	S.K.Energy(MeV)GEANT4	most prob. chg
^{40}Ar	10	621.9	545.503	14766
^{40}Ar	15	498.235	486.044	14082
^{40}Ar	20	412.234	421.272	13181
^{40}Ar	25	325.67	350.527	12065

Table 5.1: Charge Calculation Table.

5. After, surface kinetic energy versus most probable charge graphs were plotted as in Figure 5.5 for GEANT4 and FLUKA. Equation of these fitted graphs are $y = 13.9x + 7259$ and $y = 13.69x + 8675$ for GEANT4 anf

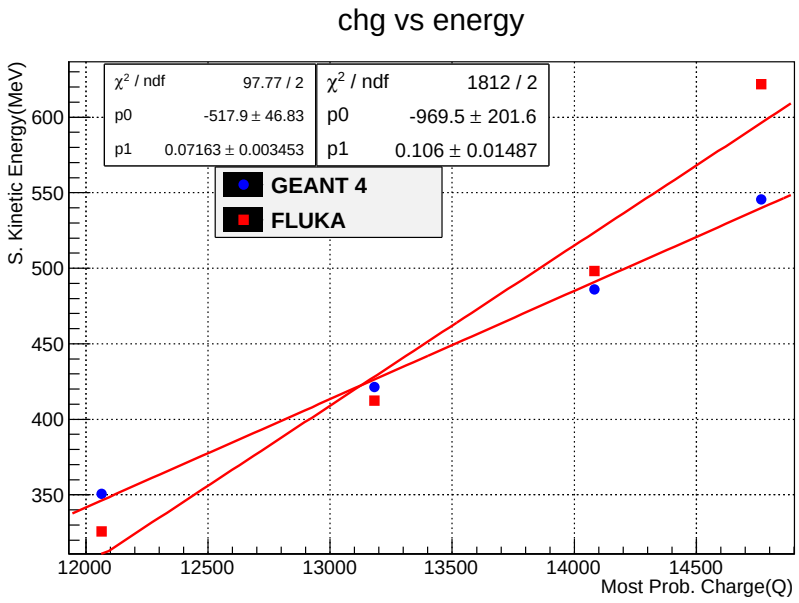

Figure 5.4: The graph shows most probable charge versus S. Kinetic Energy (MeV). Energy values are recorded by two different Monte Carlo simulations which are FLUKA and GEANT4.

Ion Type	Air 2 (cm)	Mean Charge Values	y=0.07163x-517.9 GEANT4(MeV)	y=0.106x-969.5 FLUKA(MeV)
^{40}Ar	10	14828	544.42964	602.268
^{40}Ar	15	14071	490.20573	522.026
^{40}Ar	20	13168	425.52384	426.308
^{40}Ar	25	12043	344.94009	307.058

Table 5.2: Charge Calculation Table.

FLUKA, respectively. From these equation, energy values were calculated as in Table 5.2.

6. In the next step, percentage errors in kinetic energy were calculated. // According to the calculations, they were found to be as in Table 5.3. According to Table 5.3 GEANT4 values are more accurete or more reliable than FLUKA values.

In the second part of the analysis, the differences between GEANT4 and FLUKA were compared. LET graphs and values of different simulations are shown as in Figure 5.6.

According to Table 5.4, LET values, which are recorded by GEANT4 and FLUKA, have some differences between each other with respect to using exactly

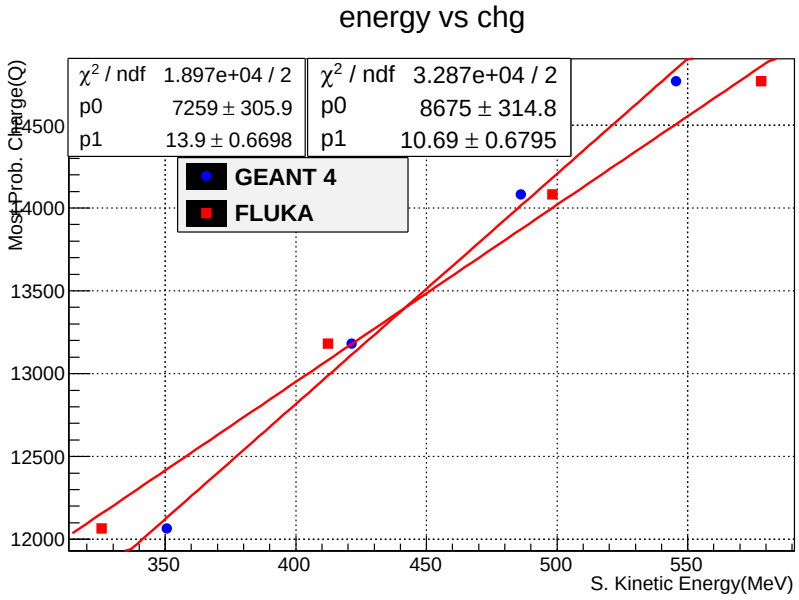

Figure 5.5: The graph shows energy versus most probable charge graph. Energy values are recorded by two different Monte Carlo simulatons which are FLUKA and GEANT4.

Ion Type	Air2(cm)	Error in MeV for GEANT4	Errors in MeV for FLUKA
^{40}Ar	10	2.49	11.99
^{40}Ar	15	2.12	10.22
^{40}Ar	20	1.87	8.39
^{40}Ar	25	1.51	6.03

Table 5.3: Error Table for Simulation Values.

Ion Type	Air2(cm)	LET(MeV/mg/cm^2)GEANT4	LET(MeV/mg/cm^2)FLUKA
^{20}Ne	20	2.55	2.63
^{40}Ar	20	10.01	10.15
^{84}Kr	10	33.71	34.81
^{129}Xe	10	61.41	69.28

Table 5.4: LET values for GEANT4 and FLUKA for this data, Air 1 is 5 cm, kapton, silion thickness are 50 μm and 1.5 cm for each ion, respectively. Scintillator thickness is 100 μm for Ne, Ar and Kr but for Xe it is 50 μm.

the same parameters. Especially, a significant increase as a function of Z number of projectile ions was noted between these different simulation. Main reason of these differences is due to physics list. Because each simulation uses different parameters during calculation of intereaction of particle with matter. Increasing Z

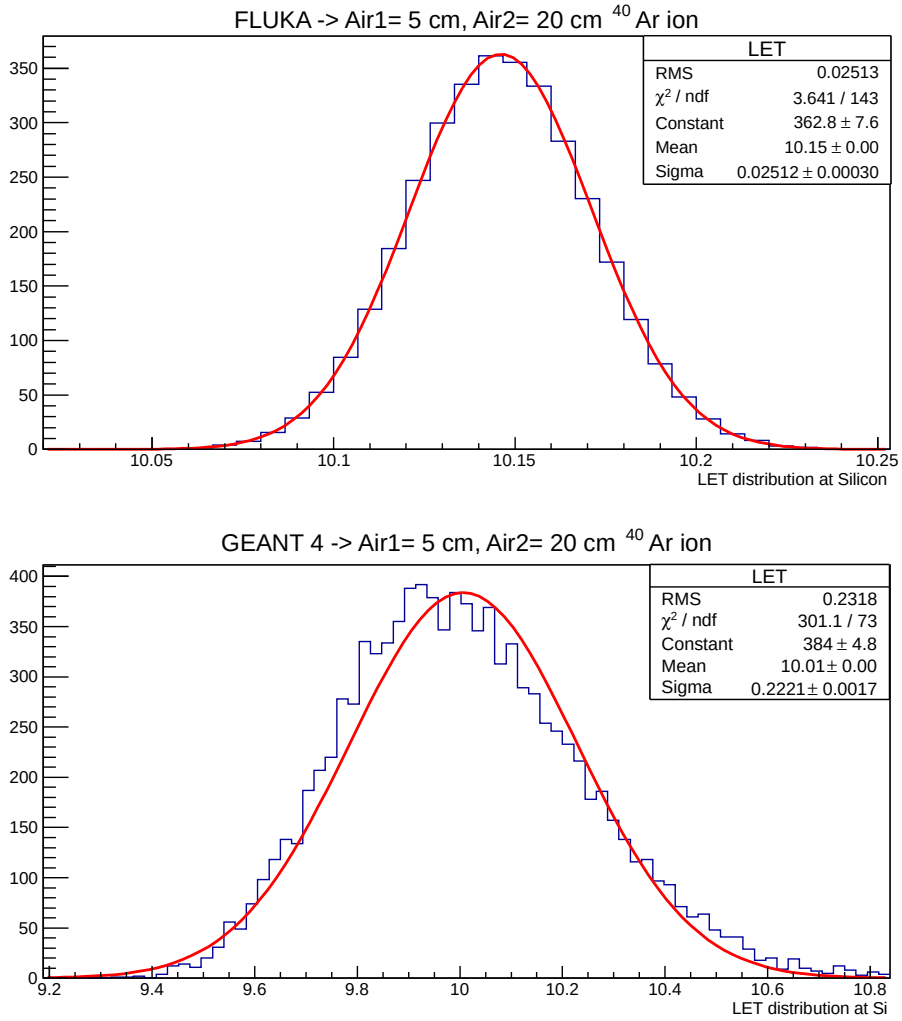

Figure 5.6: Recorded LET values from GEANT4 and FLUKA.

number causes more intereactions so that there is a significant differences between recorded LET values.

Moreover, we know that kinetic energy is directly proportional to square of atomic charge of incident particle as in Equation 5.2 [13].

$$-\left(\frac{dE}{dx}\right) = 2Pq^4Z_1^2Z_2N_{at}\left(\frac{M_2}{m}\right)\left(\frac{1}{E}\right)\left(\frac{4E}{E_{eh}}\right) \tag{5.3}$$

where Z_1 and Z_2 are atomic charges of incident particle and target material, N_{at} is the atomic density of target, M_2 the corresponding atomic mass, m and E are the mass and kinetic energy of incident particles, E_{eh} is the mean ionisation

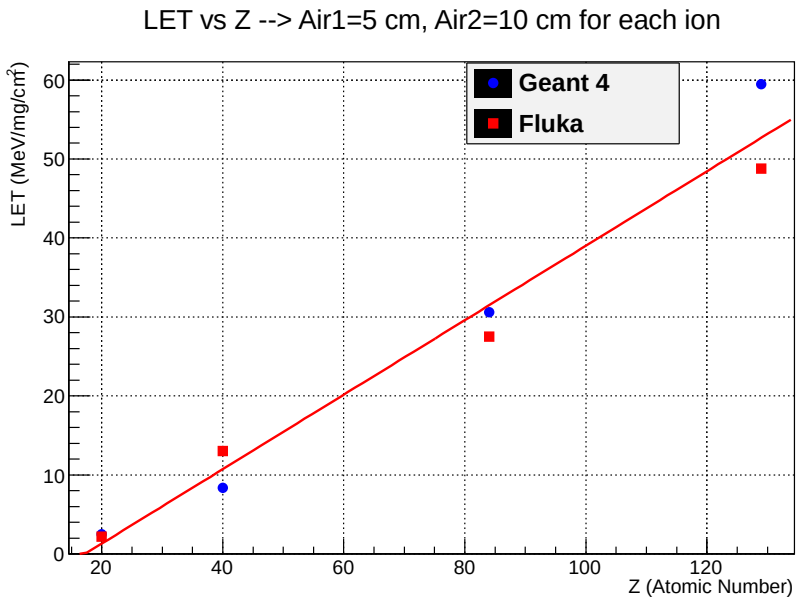

Figure 5.7: LET versus Z (atomic number) graph. Z is recorded for ^{20}Ne, ^{40}Ar, ^{84}Kr, ^{129}Xe ions. Setup parameters are Air 1 is 5 cm, Air 2 is 10 cm scintillator thikness is 100 μm, kapton thickness 50 μm and silicon thickness is 1.5 cm for each running.

energy and P is stopping number of material [13].

So, if Z^2 increases, kinetic energy value increases, too. By using Equation 5.2, relation between kinetic energy and LET can be investigated. Increase of kinetic energy values causes an increase in LET values as in Figure 5.7.

As a conlusion,

- Firstly, backside laser test was performed in MAPRad laboratories to make a general qualitative measurement aganist SEE. During laser test, DUT is scanned with laser and a lot of number of SEU were observed both analog and digital part of the device. But SEL was observed once during the irradiation. Result of laser test, irradiation was stopped to control and revise device aganist SEL.

- Test setup was simulated with two different Monte Carlo simulation codes (**GEANT4** and **FLUKA**) by chosing the reasonable LET values. These simulation values were compared with each other. Some differences were

observed because of physicslist of simulation.

- Secondly, ion beam test was performed in Catania, LNS with cyclotron accelator. Four different ion beams were used for SEE tests. Benchmark was adjusted according to simulation parameters (air1, air2, scintillator and kapton thickness).

- Before the irradiation of device, beam profile and counting of charges were investigated. During Xe ion irradiation, SEL was recorded again. As a result of this, the device was not radiation hardened.

- Measured charged data and simulation results were evaluated. FLUKA and GEANT4 data were compared respect to measured charge data. GEANT4 is more accurate than FLUKA for our test setup.

- Number of SEE in unit area (cross-section (cm^2)) is calculated by device manufacturers and by using the LET values, which were calculated by GEANT4, LET versus cross-section graph is drawn and fit with Weibull function.

- LET versus cross-section graph gives threshold and saturation LET values information. According to these values, the device is categorized whether to be used in the expected radiation environment or not.

REFERENCES

[1] M. Maher *Radiation Design Considerations Using CMOS Logic* National Semiconductor, Application Notes 924, January 1994.

[2] ESCC 25100 Single Event Effect Test Methods and Guidelines
$https://escies.org/GetFile?rsrcid=561$ Last visited June 2011.

[3] ESCC 22900 Total Dose Steady-State Irradiation Test Method
$https://escies.org/escc/specifications/22900.pdf$ Last visited June 2011.

[4] ASTM F1892 - Guide for Ionizing Radiation (Total Dose) Effects Testing of Semiconductor Devices
$http://www.astm.org/Standards/F1892.htm$ Last visited June 2011

[5] ASTM F1192 - Guide for the Measurement of Single Event Phenomena (SEP) Induced by Heavy Ion Irradiation of Semiconductor Devices
$http://www.astm.org/Standards/F1192.htm$ Last visited June 2011.

[6] J. R. Schwank, M. R. Shaneyfelt, P. E Dodd *Radiation Hardness Assurance Testing of Microelectronic Devices and Integrated Circuits: Radiation Environments, Physical Mechanisms, and Foundations for Hardness Assurance* Sandia National Laboratories Document SAND-2008.

[7] Radiation Environments, Realibity and Radiation Effects on Advanced CMOS Technologies,
$http://rreact.dei.unipd.it/Tutorials/radiation_environments.html$ Last visited July 2011.

[8] O. Amutkan *Space Radiation Environment and Radiation Hardness Assurance Tests of Electronic Components to be Used in Space Missions* METU, Phd Thesis, July 2010

[9] NASA The Radiation Environments
$http://radhome.gsfc.nasa.gov/radhome/papers/slideshow10/SC_NSREC97/sld007.htm$ Last visited July 2011.

[10] Nasa's Cosmos
$http://ase.tufts.edu/cosmos/print_images.asp?id = 29$ Last visited July 2011.

[11] I. A. Kurochkin, B. Wiegel, B.R.L. Siebert *Study of the Radiation Environments Caused by Galactic Cosmic Rays at Flight Altitudes, at the Summit of the Zugspitze and at PTB Braunschweig* Radiation Protection Dosimetry, Nuclear Technology Publishing, Vol. 83, No. 4, pp. 281â291 (1999).

[12] A. K. Sutton *Displacemnt Damage and Ionization Effects in Advanced Silicon-Germanium Heterojunction Bipolar Transistors* Master Thesis Georgia Institute of Technology, August 2005.

[13] C. Claeys, E.Simoen *Radiation Effects in Advanced Semiconductor Materials and Devices* Springer series in materials science; v. 57 2002.

[14] CREME VanderBuilt University, School of Engineering,
$https://creme.isde.vanderbilt.edu/$ Last visited July 2011.

[15] SPENVIS, Space Environments, Effects and Eduacation Systems
$http://www.spenvis.oma.be/$ Last visited July 2011.

[16] E. G. Stassinopoulos, G. J. Brucker, D. W. Nakamura, C. A. Stauffer, G. B. Gee, J. L. Barth, *Solar flare proton evaluation at geostationary orbits for engineering applications* IEEE Trans Nucl Sci 43:369-382, 1996.

[17] ESA European Space Agency, Space Science,
http : *//www.esa.int/esaSC/SEMU4QS1VED$_i$ndex$_0$.html* Last visited July 2011.

[18] R. L. Pease, A. H. Johnston, J. L. Azarewicz *Radiation Testing of Semiconductor Devices for Space Electronics* Proceedings of the IEEE, Vol. 76, No.11, November 1988.

[19] J. Janesick, T. Elliott, F. Pool *Radiation Damage in Scientific Charge-Coupled Devices* IEEE Transactions on Nuclear Science, Vol. 36, No. 1, February 1989.

[20] J. R. Srour, C. J. Marshall, and P. W. Marshall *Review of Displacement Damage Effects in Silicon Devices* IEEE Transactions on Nuclear Science, Vol. 50, No. 3, June 2003.

[21] L. Adam, A. G. Holmes-Siedle *Handbook of Radiation Effects* Oxford Scientific Publishers, Oxford 2003.

[22] Uppsala University, Svedberg Laboratory, Radiation testing page,
http : *//www.tsl.uu.se/radiation$_t$esting/tsl$_s$ee.html* Last visited July 2011.

[23] Arizona State University, Keith E. Holbert
http : *//holbert.faculty.asu.edu/eee*560*/see.html* Last visited July 2011.

[24] R. A. Reed, J. Kinnison, J. C. Pickel, S. Buchner, P. W. Marshall, S. Kniffin, and K. A. Label *Single-Event Effects Ground Testing and On-Orbit Rate Prediction Methods: The Past Present and Future* IEEE Transactions on Nuclear Science, Vol.50, No. 3 June 2003.

[25] Aerospace, Single Event Effect Testing,
http : *//www.aero.org/capabilities/seet/primer.html* Last visited July 2011.

[26] S. N. Ahmed *Physics and Enginering of Radiation Detection* Academic Press Inc. Published by Elsevier , 1st Edition 2007.

[27] W.R. Leo *Techniques for Nuclear and Particle Physics Experiments* 2nd Edition 1987.

[28] A. D. Canto *Notes on Principles and Techniques of Experimental Particle Physics* September 1 2007.

[29] C. Kreuter *Longitudinal Shower Development in the DELPHI Electromagnetic Calorimeter HPC* 21 June 1993.

[30] H. Bichsel (University of Washington), D.E. Groom (LBNL), and S.R. Klein (LBNL) *PASSAGE OF PARTICLES THROUGH MATTER* Revised April 2006.

[31] W. Leroy *Principles of Radiation Interactions in Matter and Detection* 2nd Edition World Scientific Publishing 2008.

[32] A. Das and T. Ferbel *Introduction to Nuclear and Particle Physics* December 2003.

[33] J. S. Rigden *Building blocks of matter : a supplement to the Macmillan encyclopedia of physics* 2003.

[34] C. Leroy and P. G. Rancoita *Particle interaction and displacement damage in silicon devices operated in radiation environments* IOP PUBLISHING Rep. Prog. Phys. Vol.70, pg.493â625, (2007).

[35] Electromagnetic Standard Physics Working Group
http : *//geant*4.*web.cern.ch/geant*4/*collaboration*
/working$_g$*roups/electromagnetic/* Last visited in July.

[36] B. Alpat, R. Battison, M. Bizzari, S. Blasko, D. Carrafini, L. Dimasso, G. Esposito, L. Farnesini, M. Ionica, M. Menichelli, A. Papi, G. Pontetti, V.

Postolache *A pulsed nanosecond IR laser diode system to automatically test the Single Event Efffects in the laboratory* Nuclear Instruments and Methods in Physics Research A 485 (183-187) 2002.

[37] ROOT A data Analysis Framework
http : *//root.cern.ch/drupal/*

[38] Natural Instruments, *http* : *//www.ni.com/labview/* Last visited in December 2011.

[39] R. Truscott, F. Lei, C.S. Dyer, B. Quaghebeur, D. Heynderickx, R. Nieminen, H. Evans, E. Daly *MULASSIS - Monte Carlo Radiation Shielding Simulation for Space Applications Made Easy Radiation and Its Effects on Components and Systems* RADECS 2003.

[40] F. Lei, C. S. Dyer, B. Quaghebeur, D. Heynderickx, P. Nieminen, H. Evans, and E. Daly *MULASSIS: A Geant4-Based Multilayered Shielding Simulation Tool*, IEEE Transactions on Nuclear Science, vol. 49, no. 6, December 2002.

[41] Fermilab Geant 4 Tutorial *Geant4 Physics in More Detail* Dennis Wright(SLAC), 27-29 October 2003.

[42] F. Lei, P. R. Truscott *Software User's Document for Multi Layered Shielding Simulation.*

[43] A. Ferrari, P.R. Sala, A. Fasso, and J. Ranft *Fluka: a multi-particle transport code, program version 2011*, GENEVA 2011.

[44] S. Leavy *Test Report for Single Event Effects Testing of the Performance Semiconductor (PACE) 1750A Central Processing Unit* Honeywell Space System, July 31, 1998.

[45] M. Menichelli, B. Alpat, A. Papi, R. H. Sorensen, G. A. P. Cirrone, F. Ferrera, P. Finocchiaro, M. Lattuada, D. Rifuggiato, F. Bizzarri, D. Caraffini,

M. Petasecca, F. Renzi, H. Denizli, and O. Amutkan *The Radiation Hardness Assurance Facility at INFN-LNS Catania for the Irradiation of Electronic Components in Air* IEEE Transactions on Nuclear Science, Vol. 57, No. 4, August 2010.

APPENDIX A

GEANT4 SIMULATION HIERARCHY

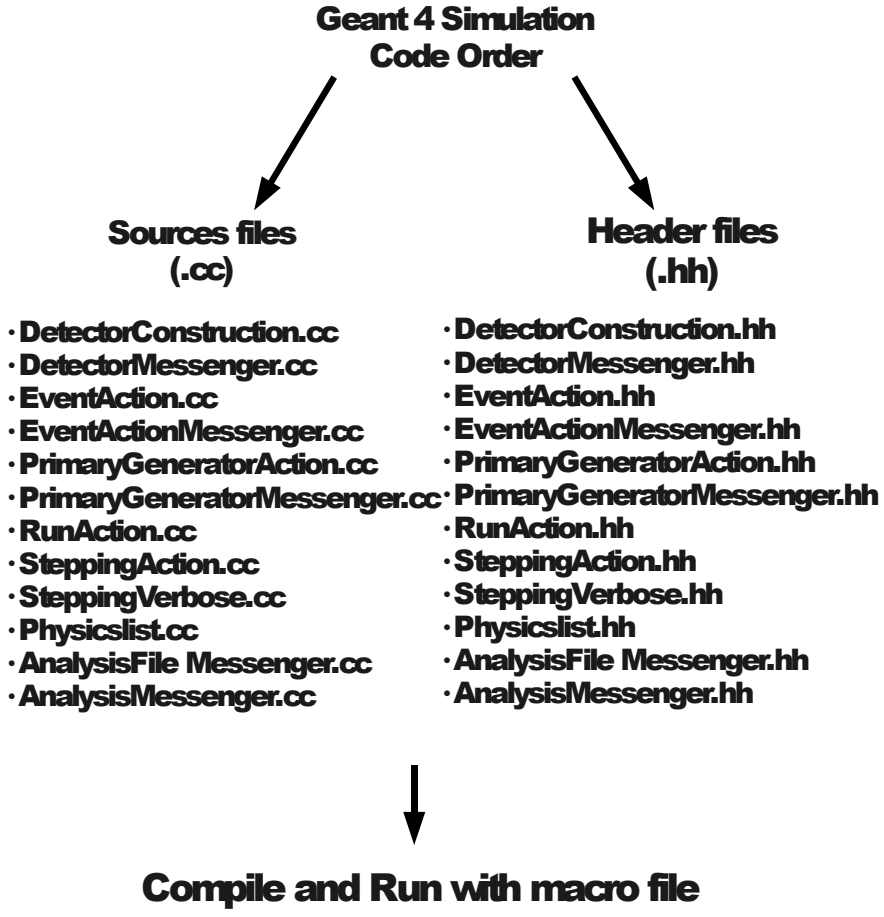

APPENDIX B

AN EXAMPLE OF MACRO FILE FOR GEANT4, MULASSIS AND GRAS

```
/control/verbose 1
/control/saveHistory lnsHistory.out
/run/verbose 0
/event/verbose 0
/tracking/verbose 0
#########################
# Set of the physic models
#
/Physics/addPhysics emstandard_opt3             # Electromagnetic model
/Physics/addPhysics Em_extra_physics
/Physics/addPhysics Elastic                     # Hadronic elastic model
/Physics/addPhysics decay
/Physics/addPhysics radioactive_decay
/Physics/addPhysics Stopping_physics
/Physics/addPhysics Neutron_tracking_cut
/Physics/addPhysics binary                      # Hadronic inelastic model
#/Physics/addPhysics local_ion_ion_inelastic    # Optional Hadronic inelastic model for ions
#########################
# Initialisation procedure
#
/run/initialize
#########################
# VISUALIZATION OPTIONS
#/vis/scene/add/eventID
#/vis/scene/add/trajectories rich
#/vis/open OGLIX
#/vis/viewer/reset
#/vis/viewer/set/viewpointThetaPhi 70 20
#/vis/drawVolume
#/vis/viewer/flush
#/vis/scene/add/trajectories
#/vis/scene/endOfEventAction accumulate
#/vis/scene/add/trajectories smooth
#/vis/modeling/trajectories/create/drawByCharge
#/vis/modeling/trajectories/drawByCharge-0/default/setDrawStepPts true
#/vis/modeling/trajectories/drawByCharge-0/default/setStepPtsSize 0
#########################
# Set here the cut and the step max for the tracking.
#
/run/setCut 1 mm
# useful for voxelized structures
#/Step/StepMax 0.01 mm

#########################
# here look at primaryGenerator.cc, z=-1. *mm
#
/gun/position 0. 0. -1. mm
/gun/direction 0. 0. 1.
/gun/particle ion
/gun/ion 10 20 0
/gun/energy 400 MeV
#########################
/run/beamOn 10000
```

APPENDIX C

LASER TEST SETUP EQUIPMENTS

PULSED DIODE LASER MODULES

Featuring peak output powers of up to 100W, these pulsed Laser Diode Modules offer pulse widths ranging from 7 to 50ns with fast rise and fall time.

ML Series:
The ML family of pulsed laser modules offers peak output powers of up to100W at 905nm. These units include the laser diode, focusing lens, and pulse drive electronics and require only a regulated DC input voltage and a TTL timing trigger to operate. ML series pulsers are ideal for applications requiring high peak pulse powers, such as rangefinding and lidar.

ILC & IPC Series
Our ILC and IPC pulsers offer peak pulse currents from 1 to 105A and pulse widths from 7 to 500ns. Available wavelengths include 850, 905, 1064, and 1550nm. ILC family contain an internal power supply that allows for either a built-in trigger pulse or a user-supplied trigger. IPC pulsers do not incorporate an internal power supply, so users must supply a trigger pulse and a bias voltage. Both series are temperature compensated to regulate output power, and both are suitable for any number of applications, including rangefinding, atmospheric communications, lidar and biomedical analysis.

MODULE SPECIFICATIONS	ML20A15	ML40H15	ML60H15	ML100H15
Dimensions, W x L x H, in. / mm	2.12 x 3.40 x 0.58 / 53.85 x 86.44 x 14.73	2.12 x 3.40 x 1.02 / 53.85x86.44x26.01	2.12 x 3.40 x 1.02 / 53.85 x 86.44 x 26.01	2.12 x 3.40 x 1.02 / 53.85x86.44x26.01
Peak Output Power (W)	20	40	60	100
Pulse Width (ns)	15	15	15	15
Max. Pulse Repetition Frequency (kHz)	10	10	6	5
Operating Voltage (VDC)	9-14.5	9-14.5	9-14.5	9-14.5
Max. Operating Current (mA)	100	150	120	150
Max. Laser Drive Current (mA)	17000	17000	20000	20000

PULSER SPECIFICATIONS		IL9C	IL10C	IL20C	IL25C	IL30C	IL40C	IL60C	IL75C
Dimensions, ϕ x L, in. / mm		1.0 x 4.0 / 25.4 x 101.6	1.0 x 4.0 / 25.4 x 101.6	1.0 x 4.0 / 25.4 x 101.6	1.0 x 4.0 / 25.4 x 101.6	1.0 x 4.0 / 25.4 x 101.6	1.25 x 4.0 / 31.75 x 101.6	1.25 x 4.0 / 31.75 x 101.6	1.25 x 4.0 / 31.75 x 101.6
Pulse Current (adjustable, A)		1-9	6-11	11-22	14-27.5	16-33	22-44	33-66	41-82.5
7-50ns Pulse Width	Rise Time (ns, typical)	2	2	3	4	4	5	5	8
	Fall Time (ns, typical)	2	3	5	6	6	7	8	10
51-200ns Pulse Width	Rise Time (ns, typical)	12	14	16	18	28	20	22	24
	Fall Time (ns, typical)	14	16	18	20	20	22	26	28
Max. Pulse Rate (kpps)	External Trigger	50	40	30	20	20	20	15	10
	Internal Clock	20	20	20	20	20	20	20	20
Propogation Delay (ns)		10	10	10	10	10	10	10	10
Supply Voltage (VDC)		12-24	12-24	12-24	12-24	12-24	12-24	12-24	12-24
Physical Diode Compatibility		9 & 5.6mm 8:32, 10:32	9 & 5.6mm 8:32, 10:32	9 & 5.6mm 8:32, 10:32	9 & 5.6mm 8:32, 10:32	9 & 5.6mm 8:32, 10:32	9 & 5.6mm 8:32, 10:32	9 & 5.6mm 8:32, 10:32	9 & 5.6mm 8:32, 10:32

Cube Beamsplitter Holders

CH-1 *CH-0.5*

- Modular, beamsplitter mounts
- Integrates beamsplitter and standard optics into a single, compact unit
- Post-mountable; compatible with 1 in. and 2 in. rotary stages

The versatility and utility of CH Series Cube Beamsplitter Holders make them an indispensable tool in the optics laboratory. Their modular design allows optics that are commonly used with beamsplitters, such as wave plates, polarizers, filters, lenses, and mirrors to be quickly attached and removed. Used in conjunction with an affordable assortment of standard 0.5 in. (12.7 mm) and 1 in. (25.4 mm) optics, the cube holders quickly convert into a broad range of general optical devices. Diagrams and sample order lists for three of the most common configurations are shown: an optical isolator, T-splitter, and variable attenuator/beamsplitter.

The cube beamsplitter holder's external thread is compatible with our RSP Series, 481-A, and RS65 Rotation Stages for precise rotation of a beamsplitter cube.

Ordering Information

Model	Description
CH-0.5	0.5 in. (12.7 mm) Cube Beamsplitter Holder
CH-1	1 in. (25.4 mm) Cube Beamsplitter Holder
MLH-0.5	0.5 in. (12.7 mm) Optic Holder
CH-PORT	Optic Adaptor for CH-0.5
LPLH-1T	1.0 in. (25.4 mm) Optic Holder

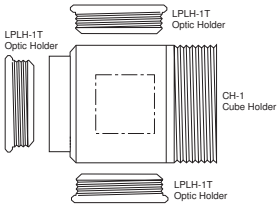

The CH-1 Beamsplitter Cube Holder's aluminum housing contains an internal 1 in. (25.4 mm) beamsplitter holder (beamsplitter not included). Ports allow optics to be positioned in beam entry and exit paths. Standard 1 in. (25.4 mm) optics may be quickly attached to Cube Holder ports using Newport LPLH-1T optic holders, which attach to the side ports.

Model CH-0.5

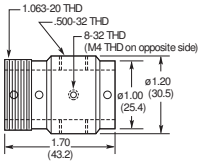

Model CH-PORT

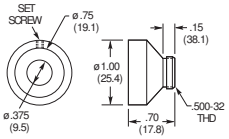

Model MLH-0.5 with Retaining Ring

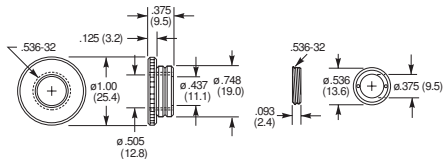

CAD

Related Products

RSP Series rotation stages (see page 912)

RS65 rotations stages (see page 911)

Broadband Non-Polarizing Cube Beamsplitters (see page 547)

Optional Set-ups

Optical Isolator

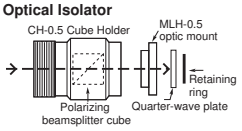

T-Splitter

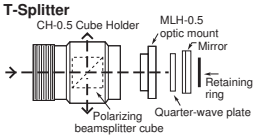

Variable Attenuator

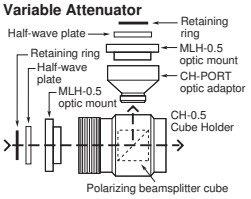

Newport Experience | Solutions
Phone: 1-800-222-6440 • Fax: 1-949-253-1680

CB-2818B

CCTV

Mini Camera

1/3" B/W Mini Camera

- **1/3" Sony CCD Image sensor**
- **450 TV Lines**
- **Min. illumination at 0.02 Lux, F 1.4**
- **3.6 mm Board Lens**
- **Auto Electronics Shutter**
- **Auto Gain Control**
- **DC 12V**
- **45(W) x 45(H) mm**
- **Ext. Model: CB-2816B/ small size: 35(W) x 35(H)mm**

Specifications	Values
Pick up Element	Sony CCD Image Sensor
Number Of Pixels	EIA>510(H)Ã—492(V) , CCIR>512(H)Ã—582(V)
Auto Electronics Shutter	ON
AGC	ON
Sync System	Internal Sync
Scanning System	2i¼š1 Interlace
resolution	450 TV Lines
S/N Ratio	More than 48dB
Gamma	0.45
Minimum Illumination	0.02 Lux, F 1.4
Horizontal Sync. Frequency	EIA> 15.734 KHz , CCIR>15.625 KHz
Video output	1.0 Vp-p, 75 ohm
Power source	DC 12V
Power Consumption	1.5 W
Operating Temperature	-10℃ to +60℃
lens Amount	3.6mm Board Lens
Shutter control	EIA> 1/60~1/100,000 sec., CCIR> 1/50~1/100,000 sec.
Dimension	45(W) Ã— 45(H) mm
Weight	0.17 kg

Beam-Displacing Prisms

Two parallel, but laterally displaced, orthogonally polarized output beams are transmitted from one unpolarized input beam when passing through a CVI Melles Griot beam-displacing prism. If the input beam is linearly polarized, the output can be made to vary continuously and sinusoidally from one parallel beam to the other by rotating the input polarization angle.

- The ordinary beam is undeviated.
- The extraordinary beam is deviated by 6 degrees within the prism.
- Upon exit, the extraordinary beam is again parallel with the input beam and the exiting ordinary beam.
- Single-layer antireflection coatings are available centered at either 550 or 830 nm.

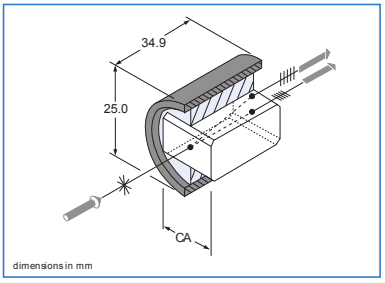

PBD beam-displacing prisms

SPECIFICATIONS: Beam-Displacing Prisms

Wavelength Range	350–2300 nm
Optical Material	Optical- or laser-grade calcite
Transmission (Ratio of Total Output to Total Unpolarized Input)	350 nm: 35–40% 400 nm: 65–70% 500 nm: 80–88% and greater at longer wavelengths
Dimension Tolerance	Outside diameter 8 0.04 mm; length 8 0.2 mm
Centration	3 arc minutes
Surface Quality	40-20 scratch and dig
Mounting	Cylindrical black-anodized aluminum housing

Beam-Displacing Prisms

CA (mm)	Beam Displacement at 500 nm (mm)	Extinction Ratio	Coating Wavelength Range (nm)	PART NUMBER FORMER‡	PART NUMBER REPLACED BY
Optical Grade					
10# 10	3.3	1# 10^4 4	Uncoated	03 PBD 001	PBD-10.0
10# 10	3.3	1# 10^4 4	425-675	03 PBD 001/A	PBD-10.0-425-675
10# 10	3.3	1# 10^4 4	670-1064	03 PBD 001/C	PBD-10.0-670-1064
Laser Grade					
10# 10	3.3	5# 10^4 5	Uncoated	03 PBD 312	PBDL-10.0
10# 10	3.3	5# 10^4 5	425-675	03 PBD 312/A	PBDL-10.0-425-675
10# 10	3.3	5# 10^4 5	670-1064	03 PBD 312/C	PBDL-10.0-670-1064

‡ Former Melles Griot part number is replaced by new CVI Melles Griot part number